

JUN 13 1947


**NACA**

# RESEARCH MEMORANDUM

for the

Bureau of Aeronautics, Navy Department

HYDRODYNAMIC CHARACTERISTICS OF A  $\frac{1}{10}$ -SIZE POWERED

DYNAMIC MODEL OF THE XP5Y-1 FLYING BOAT IN

SMOOTH WATER - LANGLEY TANK MODEL 228C-1

TED NO. NACA DE309

By

Roland E. Olson, Marvin I. Haar, and David R. Woodward

Langley Memorial Aeronautical Laboratory

Langley Field, Va.

CLASSIFIED DOCUMENT

CONTAINS PROPRIETARY  
INFORMATION

This document contains classified information affecting the National Defense of the United States within the meaning of the Espionage Act, USC 80361 and 80362. Its transmission or the revelation of its contents in any manner to an unauthorized person is prohibited by law. Information so classified may be imparted only to persons in the military and naval services of the United States, appropriate civilian officers and employees of the Federal Government who have a legitimate interest therein, and to United States citizens of known loyalty and discretion who of necessity must be informed thereof.

TECHNICAL  
EDITING  
WAIVED

## NATIONAL ADVISORY COMMITTEE FOR AERONAUTICS

WASHINGTON

NOT TO BE TAKEN FROM THIS ROOM

JUN 5 1947

NACA LIBRARY  
LANGLEY MEMORIAL AERONAUTICAL

Langley Field, Va.

CLASSIFICATION CHANGED

UNCLASSIFIED  
To

By authority of *NACA Review*  
R. V. 116  
at 7-1-57



NATIONAL ADVISORY COMMITTEE FOR AERONAUTICS

RESEARCH MEMORANDUM

for the

Bureau of Aeronautics, Navy Department

HYDRODYNAMIC CHARACTERISTICS OF A  $\frac{1}{10}$ -SIZE POWERED

DYNAMIC MODEL OF THE XP5Y-1 FLYING BOAT IN

SMOOTH WATER - LANGLEY TANK MODEL 228C-1

TEST NO. NACA DE309

By Roland E. Olson, Marvin I. Haar, and David R. Woodward

SUMMARY

An investigation of the hydrodynamic characteristics of a  $\frac{1}{10}$ -size powered dynamic model of the XP5Y-1 flying boat was made in Langley tank no. 1. At aft locations of the center of gravity, the basic model was unstable when landed at low trims (near  $5^\circ$ ). This instability was reduced by a forward movement of the center of gravity, a rearward movement of the step, an increase in plan form of the step from  $30^\circ$ -vee to  $45\frac{10}{2}^\circ$ -vee, or a reduction in the angle of afterbody keel. A reduction in the angle of afterbody keel greater than  $1^\circ$  caused excessive upper limit porpoising at high landing trims.

Stable take-offs for the basic model were possible at all practicable positions of the center of gravity and flap deflections. An increase in gross load of 21.5 percent, and an increase in forward acceleration from 1.0 to 4.5 feet per second per second had no appreciable effect on the stable range for take-off. The change in the location and plan form of the main step reduced the stable range slightly. A decrease in the angle of afterbody keel reduced the stable range approximately 2 percent mean aerodynamic chord per degree change of angle of afterbody keel.

Spray in the propellers was light at the design gross load, and was not considered excessive at a gross load of 150 pounds.

## INTRODUCTION

An investigation of the take-off and landing stability of a  $\frac{1}{10}$ -size model of the Consolidated XP5Y-1 flying boat has been made in Langley tank no. 1. The XP5Y-1 is a four-engine, 123,500-pound, long-range flying boat, designed to operate at a cruising speed considerably higher than that of most contemporary flying boats. This design is of particular interest in that relatively high wing loading, low power loading, and high length-beam ratio are used.

The investigation was requested by the Bureau of Aeronautics, Navy Department, in their letter dated July 18, 1946, Aer-DE-31, 52931.

The principal purpose of this report is to make the hydrodynamic data most pertinent to this particular airplane immediately available to the Bureau of Aeronautics, Navy Department, and the Consolidated Vultee Aircraft Corporation. The take-off and landing characteristics of the basic model are presented together with data for several modifications that improved the landing characteristics. All of the modifications represent changes external to the basic model.

Messrs. E. G. Stout and F. L. Thornburg of the Consolidated Vultee Aircraft Corporation witnessed most of the tests.

## SYMBOLS

$C_L$	aerodynamic lift coefficient $\left( \frac{\text{Lift}}{\frac{1}{2}\rho S V^2} \right)$
$C_m$	aerodynamic pitching-moment coefficient $\left( \frac{M}{\frac{1}{2}\rho S V^2 \bar{c}} \right)$
$T_e$	effective thrust, pounds $(T - \Delta D = D_o + R)$
where	
$\bar{c}$	mean aerodynamic chord (M.A.C.), feet
$D_o$	drag of model without propellers, pounds
$\Delta D$	increase in drag due to slipstream, pounds

M	aerodynamic pitching moment, pound-feet
R	measured resultant horizontal force with power on, pounds
$\rho$	density of air, slugs per cubic foot
S	area of wing, square feet
T	propeller thrust, pounds
V	carriage speed, feet per second (approximately 95 percent of airspeed)

Other symbols are:

$\delta_e$	elevator deflection, degrees
$\delta_f$	flap deflection, degrees
$\delta_s$	stabilizer setting, degrees
$\tau$	trim, degrees (angle between base line of hull and water plane)
$\tau_L$	landing trim at contact with water, degrees

#### DESCRIPTION OF MODEL

The  $\frac{1}{10}$ -size powered dynamic model used in the investigation was designed and constructed by the Consolidated Vultee Aircraft Corporation. A photograph of the model on the towing apparatus in Langley tank no. 1 is shown in figure 1, and a three-view drawing of the basic configuration, designated Langley tank model 228C-1, is shown in figure 2. Pertinent dimensions of model 228C-1 are given in table 1.

The design of the hull is described in reference 1. It had a forebody length-beam ratio of 5.8 and an afterbody length-beam ratio of 4.2, making an over-all hydrodynamic ratio of 10.0. The forebody bottom was straight for approximately  $\frac{2}{3}$  beam forward of the step centroid and the dead rise increased rapidly at forward stations to form an extremely sharp bow. The angle of dead rise of the straight forebody and the afterbody was  $22\frac{1}{2}^\circ$ . The step had a  $30^\circ$ -vee plan form with its centroid at 31.3 percent of the projected mean aerodynamic chord and a depth at the centroid of 14.2 percent beam. The angle between the forebody and afterbody keels was  $6.5^\circ$ .

The following modifications were investigated:

Model 228D-1. - Basic model with step moved aft 0.89 inch, 4.5 percent mean aerodynamic chord. The depth of step at the centroid was increased from 14.2 percent beam to 15.0 percent beam by this change. (See fig. 3(a).)

Model 228H. - Step plan form of basic model increased to  $45\frac{1}{2}^\circ$ -vee by adding blocks to the original  $30^\circ$ -vee. The depth of step at the chine was the same as that of the basic model. The depth at the centroid and the position of the centroid were the same as those of model 228D-1. (See fig. 3(b).)

Model 228G-1. - Basic model with  $5\frac{1}{2}^\circ$  angle of afterbody keel. (See fig. 3(c).)

Model 228J-1. - Basic model with  $4\frac{1}{2}^\circ$  angle of afterbody keel. (See fig. 3(c).)

Model 228I. - Basic model with depth of step at the centroid reduced from 14.2 percent beam to 11.7 percent beam and a  $5^\circ$  angle of afterbody keel. (See fig. 3(d).)

#### APPARATUS AND PROCEDURE

The apparatus and general procedures used for testing powered dynamic models are described in references 2 and 3.

The propellers were set at a blade angle of  $10.0^\circ$  at the  $3/4$  radius and rotated at 5250 rpm to provide take-off thrust. The effective thrust was measured at  $0^\circ$  trim, flaps at  $0^\circ$ , and the step 8.0 inches above the water. This thrust is shown in figure 4 together with that corresponding to the full-size thrust as estimated by Consolidated Vultee Aircraft Corporation.

In order to provide data from which the approximate load on the water could be estimated, the aerodynamic lift and pitching moment were measured with the model in the same position as that used for determination of the effective thrust. Data were obtained with and without power for two stabilizer settings ( $0^\circ$  and  $-2^\circ$  to the base line) and several flap and elevator deflections. The pitching moments were referred to a center-of-gravity location of 25 percent mean aerodynamic chord. The aerodynamic lift and pitching-moment coefficients, power off, are plotted in figure 5. The pitching-

moment coefficients with  $20^\circ$  flaps, and neutral elevators, power off, and with ground effect, estimated by Consolidated Vultee Aircraft Corporation, are also plotted in figure 5.

The aerodynamic lift and pitching moment, with power, are plotted in figure 6. On the basis of these tests a stabilizer setting of  $-1^\circ$  was used for the remainder of the investigation.

The landing stability was determined by flying the model at a desired landing trim and then uniformly decelerating the towing carriage (rate of deceleration, approximately 2 feet per second per second) to simulate the landing maneuver. The variation of trim, vertical position (rise), and speed were electrically recorded. The rise was set at zero with the model at zero trim and with the step just touching the water. A contact was installed at the step to electrically record the points at which the step entered and left the water. A similar contact indicated the point at which the sternpost first touched the water when landed at high trims. The tests were made with  $1/4$  thrust and flaps deflected  $50^\circ$  (gap at top surface taped) and a normal gross load of 123.5 pounds.

The trim limits of stability were obtained with full thrust and take-off flaps ( $20^\circ$ ).

The range of stable position of the center of gravity was determined by making take-offs with full power at a constant rate of acceleration of 1.0 foot per second per second and flaps deflected  $20^\circ$ . On the basic configuration, the center-of-gravity limits were also obtained at an acceleration of 4.5 feet per second per second, and for several elevator deflections, gross loads, and flap deflections.

With take-off power, flaps deflected  $20^\circ$ , and the center of gravity at 30 percent mean aerodynamic chord, the excess thrust was measured for model 228C-1 at hump speeds for gross loads of 123.5, 135.0, and 150.0 pounds and elevator deflections of  $0^\circ$  and  $-10^\circ$ . This excess thrust is the net accelerating force for the model.

The spray characteristics were observed during take-off and landing runs. The range of speeds over which spray struck the propellers and flaps was determined for model 228D-1 during slowly accelerated runs (rate of acceleration approximately 0.5 foot per second per second). Photographs of spray were obtained for model 228J-1.

## RESULTS AND DISCUSSION

The hydrodynamic characteristics of model 228C-1 (basic model) were determined in detail. Sufficient data were obtained for each of the modifications to show the effect of the change and to provide corrections that can be applied to the more detailed results for the basic model.

[REDACTED]

Of the hydrodynamic characteristics determined during this investigation, the landing stability appeared to be of first importance; the modifications were included in the program principally because of their effect on the landing stability.

### Landing Stability

The landing behavior of each of the configurations is presented as a landing record showing the variation of trim, rise, and forward speed with time for typical landings at trims from  $3^\circ$  to  $14^\circ$ . These results are summarized as a plot against trim at first contact of the number of skips (main step leaves the water), and the maximum and minimum trim and rise that occurred during the greatest oscillation encountered in the landing. The model designations, identifying descriptions, and figure numbers are presented in the following table:

Model	Identification	Center of gravity, percent M.A.C.	Landing record, figure	Summary plot, figure
228C-1	Basic model, $6\frac{1}{2}^\circ$ keel angle	34, 30, 26	7(a), 7(b), 7(c)	8(a), 8(b), 8(c)
228D-1	Step moved aft	34	9	10
228H	Step plan form, $45\frac{1}{2}^\circ$ -vee	34	11	12
228G-1	$5\frac{1}{2}^\circ$ keel angle	34	13	14
228J-1	$4\frac{1}{2}^\circ$ keel angle	34	15	16
228I	$5^\circ$ keel angle, shallow step	34	17	18

Basic model (model 228C-1). - With the center of gravity at 34 percent mean aerodynamic chord the model was violently unstable when landed at trims near  $5^\circ$  (figs. 7(a) and 8(a)). As many as six skips were recorded on these landings; this skipping was accompanied by large changes in rise (7 inches above the water) and by large changes in trim ( $10^\circ$ ) with a maximum trim of approximately  $14^\circ$ .

With the center of gravity at 30 percent mean aerodynamic chord (figs. 7(b) and 8(b)) the motion of the model was less violent than that at 34 percent mean aerodynamic chord; a maximum instability appeared as a change in rise at landing trims of approximately  $5^\circ$ , but only two skips occurred.

The results obtained with the center of gravity at 26 percent mean aerodynamic chord are presented in figures 7(c) and 8(c). Curves for landings at 30 and 34 percent mean aerodynamic chord are also included in figure 8(c). With the center of gravity at 26 percent mean aerodynamic chord, the motion of the model was less violent than that at 30 percent mean aerodynamic chord. The maximum change in rise again appeared at trims near  $5^\circ$ , but the number of skips was reduced to one. One skip also occurred when the model was landed without an afterbody (deep step). Inasmuch as the one skip appeared to be an inherent characteristic of the forebody, and since the changes in trim and rise were not large with the center of gravity located at 26 percent mean aerodynamic chord, these landings were considered satisfactory.

At high landing trims the stability was considered satisfactory at all positions of the center of gravity.

Effect of moving the step aft (model 228D-1). - The landing stability of the model with the step moved aft is shown in figure 10 and compared with that of the basic model and that of the model without an afterbody. The violent instability that occurred for the basic model at landing trims near  $5^\circ$  is greatly reduced. The results for model 228D-1 compare favorably with those obtained for the model without an afterbody (deep step). Landings of model 228D-1 were considered satisfactory. The after movement of the step increased the landing stability, (1) by increasing the depth of step, and (2) by effectively increasing the relative distance between the center of gravity and the step.

Effect of change in step plan form (model 228H). - The results for model 228H are compared in figure 12 with those of the basic model. Results for model 228D-1 are also included in figure 12 inasmuch as the depth of step at the centroid and the position of the centroid were the same as those for model 228H. The instability that appeared at landing trims near  $5^\circ$  for the basic model did not occur for model 228H. The results with a  $30^\circ$ -vee step (model 228D-1) and a  $45\frac{1}{2}^\circ$ -vee step (model 228H) were quite similar. Landing stability of model 228H was considered satisfactory.

Effect of change in angle of afterbody keel, constant depth of step (models 228C-1, 228G-1, 228J-1). - A summary plot of the landing characteristics for the model with an angle of afterbody keel of  $4\frac{1}{2}^\circ$  (model 228J-1) is shown in figure 16 together with curves of similar data for models with angles of afterbody keel of  $6\frac{1}{2}^\circ$  (model 228C-1) and  $5\frac{1}{2}^\circ$  (model 228G-1). The violence of the skipping

at low landing trims (near  $5^\circ$ ) was reduced with decrease in angle of afterbody keel. This trend has been noted during tests of other models having conventional length-beam ratios. Although the stability at low landing trims was improved by decrease in angle of afterbody keel, stability at high landing trims was impaired. With a  $6\frac{1}{2}^\circ$  angle of afterbody keel, some upper limit porpoising occurred when landing trims exceeded  $13^\circ$ . With a  $5\frac{1}{2}^\circ$  angle of afterbody keel this porpoising appeared at landing trims above  $12^\circ$ , and with a  $4\frac{1}{2}^\circ$  angle of afterbody keel, at landing trims above  $10^\circ$ . The degree of this instability is best illustrated by comparison of the landing records of figures 7(a), 13, and 15. A decrease in the angle of afterbody keel lowers the upper trim limit of stability and upper limit porpoising during landings at high trims becomes a problem with too low an angle of afterbody keel.

The model with an angle of afterbody keel of  $5\frac{1}{2}^\circ$  represented the most satisfactory compromise for the three configurations on the basis of landing stability at trims below  $12^\circ$ . With higher angles of afterbody keel than  $5\frac{1}{2}^\circ$ , skipping was violent at landing trims near the angle of afterbody keel; with lower angles of afterbody keel than  $5\frac{1}{2}^\circ$ , upper limit porpoising occurred at high landing trims. A comparison of these data with those presented in figures 10 and 12 shows that the number of skips, and the change in trim and rise during landings of the model with a  $5\frac{1}{2}^\circ$  angle of afterbody keel are greater than those for the model with the step moved aft (model 228D-1) and the model with a  $4\frac{1}{2}^\circ$ -vee step (model 228H).

Effect of a reduction in angle of afterbody keel and depth of step (model 228I).—The landing records for model 228I (fig. 17) show that landings at low trims were relatively stable but, at landing trims above  $10\frac{1}{2}^\circ$ , upper limit porpoising becomes an important consideration. Inasmuch as a decrease in depth of step and angle of afterbody keel both tend to lower the upper trim limits, this upper limit porpoising may be expected at high landing trims.

The similarity between the behavior of model 228I and model 228J-1, which has approximately the same sternpost angle, is shown in the summary plot (fig. 18). The landing stability of model 228I was not considered satisfactory because of the upper limit porpoising at high trims.

### Take-Off Stability

The variation of the trim with speed (trim tracks) was determined for each of the models. The maximum amplitude of porpoising was determined during the take-off runs and plotted against position of the center of gravity. From such plots, the forward and after limits for stable positions of the center of gravity were determined with various deflections of the elevators. An amplitude of porpoising of  $2^\circ$  was assumed to be the maximum permissible amplitude for adequate take-off stability. Positions of the center of gravity between the forward and after limits were designated as the stable range.

An oscillation in pitch, due to spray striking the horizontal tail, was observed at trims between the trim limits of stability. The amplitude of this oscillation varied from  $\frac{1}{2}^\circ$  to almost  $2^\circ$ , but generally was approximately  $1^\circ$ . On the figures showing the take-off trim tracks, vertical hatch lines are used to indicate this oscillation. Actual upper or lower limit porpoising of less than  $1^\circ$  amplitude is shown with a porpoising loop enclosing the vertical hatch lines.

The trim limits of stability, both lower and upper, were determined on the basic configuration, model 228C-1, at the design gross load of 123.5 pounds and flaps deflected  $20^\circ$  (take-off position); the upper limits were also determined with zero flaps. Complete trim limits were obtained for subsequent modifications with the exception of models 228G-1 and 228I. The trim limits for the latter two configurations were estimated by interpolation and extrapolation respectively. Wherever available, the trim limits of stability have been superimposed on typical take-off trim tracks so that the relation of the trim limits to the trim tracks with neutral and up elevators, and at forward and aft locations of the center of gravity can be seen.

Figures showing the results of the take-off investigation, together with the model numbers, are presented in the following table:

Model	Gross load, (lb)	Flap deflection (deg)	Acceleration (ft/sec <sup>2</sup> )	Figure numbers		
				Trim tracks	Maximum amplitude	c.g. limits
228C-1	123.5	0	1.0	19(a)	20(a)	20(b)
		20	1.0	19(b)	20(a)	20(b)
		40	1.0	19(c)	20(a)	20(b)
	136.0	20	1.0	21	22(a)	22(b)
	150.0	20	1.0	21	22(a)	22(b)
	123.5	20	4.5	23	24(a)	24(b)
228D-1	123.5	20	1.0	25(a)	25(b)	----
228H	123.5	20	1.0	26(a)	26(b)	----
228G-1	123.5	20	1.0	27(a)	27(b), 29(a)	29(b)
228J-1	123.5	20	1.0	28(a)	28(b), 29(a)	29(b)
228I	123.5	20	1.0	30(a)	30(b)	----

Basic model (228C-1). - Take-offs were possible at positions of the center of gravity from 21 percent to 36 percent mean aerodynamic chord with deflections of the flaps of 0°, 20°, and 40° (fig. 19). With flaps deflected 40° and at forward positions of the center of gravity, up elevators were required in order to avoid lower limit porpoising and to trim up for take-off at high speeds. With the center of gravity located at 22 percent mean aerodynamic chord and elevators deflected -15°, the model took off at a trim of 6.4° and a speed of 47 feet per second.

The effect of flaps and elevators on the range of stable position of the center of gravity is shown in figure 20(b). The forward and after limits of the center of gravity at which take-off stability is adequate can be determined from this figure for any combination of elevator and flap deflection.

The effect of load on the range of stable position of the center of gravity is shown in figure 22(b). An increase in gross load of 21.5 percent (from 123.5 pounds to 150.0 pounds) moved both limits forward approximately 1 percent mean aerodynamic chord.

An increase in acceleration had no appreciable effect on the trim tracks at speeds where the model was stable (fig. 23). When porpoising occurred, the frequency of the porpoising motion was approximately the same at rates of acceleration of 1.0 and 4.5 feet per second per second. Consequently, over the speed range where the trim track crossed the trim limit of stability, fewer cycles of porpoising occurred for the high acceleration than for the low acceleration. An increase in acceleration from 1.0 to 4.5 feet

per second per second effectively shifted the forward limit forward approximately 1.0 percent mean aerodynamic chord, and the after limit aft 0.5 percent mean aerodynamic chord (fig. 24(b)).

The static trim for the basic model at the design gross load was varied from  $4.1^\circ$  at the forward center of gravity to  $5.1^\circ$  at the most after center of gravity.

Effect of moving the step aft (model 228D-1). - An after movement of the step of 0.89 inch (4.5 percent mean aerodynamic chord), shifted the forward and after limits of stability aft by 3 and 2 percent mean aerodynamic chord, respectively, when compared with corresponding curves for the basic model 228C-1 (fig. 25(b)). Similar movement of the stable limits has been observed on other models when the position of the step has been changed.

The trim limits of stability for models 228D-1 and 228C-1 were approximately the same.

Effect of change in step plan form (model 228H). - A change in step plan form from  $30^\circ$ -vee step (model 228D-1) to a  $45\frac{1}{2}^\circ$ -vee step (model 228H) had no appreciable effect on the trim tracks, trim limits of stability or stable range of the center of gravity for take-off (fig. 26).

The static trims of model 228H were approximately the same as those of the basic model (228C-1).

Effect of change in the angle of afterbody keel with constant depth of step (models 228C-1, 228G-1, and 228J-1). - A decrease in the angle of afterbody keel moved both the low-speed peak of the lower trim limit of stability and the trim tracks in the displacement and hump speed range to lower trims. Inasmuch as both the lower trim limit and the trim tracks were shifted in the same direction, the forward limit for positions of the center of gravity for stable take-off was not affected appreciably by changes in the angle of afterbody keel. A decrease in the angle of afterbody keel from  $6.5^\circ$  to  $4.5^\circ$  moved the forward limit forward approximately 1 percent mean aerodynamic chord (fig. 29). The forward limit was not determined for the model with a  $5.5^\circ$  angle of afterbody keel (model 228G-1).

A decrease in the angle of afterbody keel moved the upper trim limits of stability to lower trims, but did not have any appreciable effect on the trim tracks at high speeds. Consequently, the after limit of the stable range was shifted forward, as the angle of afterbody keel was reduced. A decrease in the angle of afterbody keel

from  $6.5^\circ$  to  $4.5^\circ$  moved the after limit forward 5.0 percent mean aerodynamic chord (fig. 29). In summary, a decrease in the angle of afterbody keel of  $2^\circ$  (from  $6.5^\circ$  to  $4.5^\circ$ ) decreased the range of position of the center of gravity for stable take-off 4 percent mean aerodynamic chord, principally by moving the after limit forward.

With the center of gravity located at 30 percent mean aerodynamic chord, the static trim varied from  $4.8^\circ$  to  $3.7^\circ$  as the angle of afterbody keel was changed from  $6.5^\circ$  to  $4.5^\circ$ .

Effect of a reduction in angle of afterbody keel and depth of step (model 228I). - A reduction in angle of afterbody keel from  $6.5^\circ$  (with a 14.2-percent beam depth of step at the centroid) to  $5.0^\circ$  (with an 11.7-percent beam depth of step at the centroid) moved the forward and aft limits forward approximately 1 percent and 4 percent mean aerodynamic chord, respectively, which resulted in a net decrease of 3 percent mean aerodynamic chord in the range of stable position of the center of gravity (fig. 30(b)). This reduction was very nearly the same as that which would be expected for a change in afterbody keel alone (fig. 29).

The static trims of model 228I were approximately  $1.0^\circ$  less than the static trims of model 228C-1.

#### Take-Off Performance

The excess thrust, available for acceleration in the speed range near the hump (maximum resistance) with the propellers developing the scale effective thrust, was determined for model 228C-1. The excess thrust and trim at the design gross load, with two deflections of the elevators, and at two overloads are presented in figure 31. These curves have been plotted so that they have the same general shape as the resistance curves used for take-off computations. At the design gross load of 123.5 pounds the net accelerating force at the hump was approximately 6 pounds. At an overload gross load of 150 pounds, excess thrust was not available for accelerating over the hump.

#### SPRAY CHARACTERISTICS

Detailed spray observations and photographs were made for a few of the modifications. In the load range of interest for this design the spray characteristics, in general, were not greatly

different for the various models. These data, therefore, are presented in order to give an over-all evaluation of the spray characteristics.

Photographs of the bow spray of model 228J-1 are presented in figure 32. The range of speeds over which spray entered the propellers of model 228D-1 is presented in figure 33(a). It is apparent that propeller spray in smooth water will be no problem at the design load. For model 228D-1, spray in the propellers did not appear to be excessive at a gross load of 150 pounds.

The range of speed over which spray struck the flaps of model 228D-1 is shown in figure 33(b). Most of the spray struck that portion of the flaps near the inboard engines.

Spray wetted the tail turret at speeds from 14 to 21 feet per second. A typical photograph showing the spray around the tail turret is presented in figure 34. The roach from under the afterbody followed the curved sides of the tail extension and tail turret and, for a very short speed range, water was over the top of the guns.

During take-off, the forebody blister wetted the horizontal tail at speeds above 20 feet per second. (See fig. 35.) This spray, which was broken up by the action of the slipstream, was not heavy. During the landing run out, however, the slipstream did not break up this blister (1/4 take-off thrust) and consequently, a heavy jet of water struck the tail. (See fig. 35.) At high speed, intermittent spray on the horizontal tail often caused a small oscillation in trim (less than  $2^\circ$ ) during take-off. This spray is shown in the photographs of figure 36.

### CONCLUSIONS

The tank investigation of the powered dynamic model of the XP5Y-1 flying boat indicated that:

1. At aft locations of the center of gravity the basic model was unstable when landed at low trims (near  $5^\circ$ ).
2. A forward movement of the center of gravity, a rearward movement of the step, or a change in step plan form from  $30^\circ$ -vee to  $45\frac{10}{2}$ -vee produced satisfactory landing stability.
3. A decrease in angle of afterbody keel improved the landing stability at low trims, but increased the tendency toward upper limit porpoising at high trims.

4. Stable take-offs for the basic model were possible at all practicable positions of the center of gravity and flap deflections. An increase in gross load of 21.5 percent, and an increase in forward acceleration from 1.0 to 4.5 feet per second per second had no appreciable effect on the stable range for take-off.

5. An after movement of the step shifted both the forward and aft limits of stability aft and reduced the stable range slightly.

6. A change in step plan form to  $45\frac{1}{2}^\circ$ -vee had no appreciable effect on the take-off stability when compared with a modification having a  $30^\circ$ -vee step with the same depth and position at the centroid.

7. A decrease in the angle of afterbody keel reduced the stable range for take-off approximately 2 percent mean aerodynamic chord per degree change of angle of afterbody keel, principally by moving the after limit forward.

8. The amount of spray in the propellers was satisfactory at the design gross load, and did not appear excessive when the gross load was increased 21.5 percent.

Langley Memorial Aeronautical Laboratory  
National Advisory Committee for Aeronautics  
Langley Field, Va.

*Roland E. Olson*

Roland E. Olson  
Physicist

*Marvin I. Haar*

Marvin I. Haar  
Mechanical Engineer

*David R. Woodward*

David R. Woodward  
Engineering Aide

Approved:

*John B. Parkinson*  
John B. Parkinson

Chief of Hydrodynamics Research Division

## REFERENCES

1. Stout, E. G., and Fuller, R. D.: Hydrodynamic Design of the Consolidated Vultee Navy Long Range Patrol Seaplane. Rep. No. ZH-030, Consolidated Vultee Aircraft Corp., March 1946.
2. Olson, Roland E., and Land, Norman S.: The Longitudinal Stability of Flying Boats as Determined by Tests of Models in the NACA Tank. I - Methods Used for the Investigation of Longitudinal-Stability Characteristics. NACA ARR, Nov. 1942.
3. Truscott, Starr, and Olson, Roland E.: The Longitudinal Stability of Flying Boats as Determined by Tests of Models in the NACA Tank. II - Effect of Variations in Form of Hull on Longitudinal Stability. NACA ARR, Nov. 1942.

TABLE 1

## DIMENSIONS OF BASIC MODEL 228C-1

## Hull:

Maximum beam, in. . . . .	12.0
Length:	
Forebody, bow to centroid of main step, in. . . . .	69.60
Length-beam ratio . . . . .	5.8
Afterbody, centroid of main step to sternpost, in. . . . .	50.40
Length-beam ratio . . . . .	4.2
Tail extension, sternpost to aft perpendicular, in. . . . .	31.7
Over all, bow to aft perpendicular, in. . . . .	151.7
Forebody flat, beams from centroid. . . . .	2/3
Depth of step, (30°-vee):	
At keel, in. . . . .	1.95
At keel, percent beam . . . . .	16.2
At centroid, in. . . . .	1.70
At centroid, percent beam . . . . .	14.2
Step location at centroid, percent M.A.C. . . . .	31.3
Angle of forebody keel to base line, deg . . . . .	0
Angle of afterbody keel to base line, deg . . . . .	6.5
Angle of dead rise of forebody, at step (excluding chine flare), deg . . . . .	22.5
Angle of dead rise of afterbody, deg . . . . .	22.5
Height of center of gravity above base line, in. . . . .	17.21

## Wing:

Area, sq ft . . . . .	21.0
Span, ft . . . . .	14.5
Root chord, in. . . . .	26.1
Tip chord, in. . . . .	8.7
Angle of wing incidence to base line, deg . . . . .	5.0
Mean aerodynamic chord, M.A.C., in. . . . .	18.9
Leading edge M.A.C., aft of bow, in. . . . .	61.3
Leading edge M.A.C., above base line, in. . . . .	22.2
Aspect ratio . . . . .	10.0
Flaps:	
Deflection for take-off, deg . . . . .	20
Deflection for landing, deg . . . . .	50 (taped)

## Horizontal tail:

Span, ft . . . . .	5.5
Chord, in. . . . .	17.2
Area, stabilizer, sq ft . . . . .	3.3
Area, elevator, sq ft . . . . .	1.8
Total area, sq ft . . . . .	5.1
Angle of stabilizer setting to base line, deg . . . . .	-1.0

TABLE 1 - Concluded

## DIMENSIONS OF BASIC MODEL 228C-I - Concluded

## Vertical tail:

Total area, sq ft . . . . .	2.5
-----------------------------	-----

## Propeller:

Blades . . . . .	4
Diameter, in. . . . .	18.1
Blade angle ( $3/4$ radius), deg . . . . .	10
rpm at full power . . . . .	5250
Angle of thrust line to base line, deg . . . . .	7.0

Normal gross load, lb . . . . .	123.5
---------------------------------	-------

NATIONAL ADVISORY COMMITTEE FOR AERONAUTICS

FIGURE LEGENDS

Figure 1.- Model 228C-1 on towing apparatus.

Figure 2.- Model 228C-1. General Arrangement. (Dimensions in inches.)

Figure 3.- Modifications to basic model 228C-1.

(a) Model 228D-1. Step moved aft.

(b) Model 228H.  $45\frac{1}{2}^\circ$  - vee planform of step.

Figure 3.- Concluded.

(c) Models 228G-1 and J-1. Angle of afterbody reduced.

(d) Model 228I. Depth of step and angle of afterbody keel reduced.

Figure 4.- Variation of effective thrust with speed. Trim,  $0^\circ$ ;  $\delta_F = 0^\circ$ ;  
 $\delta_e = 0^\circ$ ;  $\delta_s = -2^\circ$ .

Figure 5.- Aerodynamic lift and pitching-moment coefficients, power off.

Figure 6.- Aerodynamic lift and pitching moment. Take off power; flap deflection,  $20^\circ$ .

(a) Elevator deflection,  $0^\circ$ .

Figure 6.- Continued.

(b) Elevator deflection,  $-15^\circ$ ; stabilizer setting,  $0^\circ$ .

Figure 6.- Concluded.

(c) Elevator deflection,  $-20^\circ$ ; stabilizer setting,  $0^\circ$ .

Figure 7.- Model 228C-1. Time histories of landings.

(a) Center of gravity, 34 percent M.A.C.

Figure 7.- Continued.

(a) Center of gravity 34 percent M.A.C.

Figure 7.- Continued.

(b) Center of gravity, 30 percent M.A.C..

## FIGURE LEGENDS - Continued

Figure 7.- Continued.

(b) Center of gravity, 30 percent M.A.C.

Figure 7.- Concluded.

(c) Center of gravity, 26 percent M.A.C.

Figure 8.- Model 228C-1. Number of skips and maximum and minimum trim and rise during landing.

(a) Center of gravity, 34 percent M.A.C.

Figure 8.- Continued.

(b) Center of gravity, 30 percent M.A.C.

Figure 8.- Concluded.

(c) Center of gravity, 26 percent M.A.C.

Figure 9.- Model 228D-1. Time histories of landings. Center of gravity, 34 percent M.A.C.

Figure 10.- Model 228D-1. Number of skips and maximum and minimum trim and rise during landing. Center of gravity, 34 percent M.A.C.

Figure 11.- Model 228H. Time histories of landings. Center of gravity, 34 percent M.A.C.

Figure 12.- Model 228H. Number of skips and maximum and minimum trim and rise during landing. Center of gravity, 34 percent M.A.C.

Figure 13.- Model 228G-1. Time histories of landings. Center of gravity, 34 percent M.A.C.

Figure 14.- Model 228G-1. Number of skips and maximum and minimum trim and rise during landing. Center of gravity, 34 percent M.A.C.

Figure 15.- Model 228J-1. Time histories of landings. Center of gravity, 34 percent M.A.C.

Figure 16.- Model 228J-1. Number of skips and maximum and minimum trim and rise during landing. Center of gravity, 34 percent M.A.C.

## FIGURE LEGENDS - Continued

Figure 17.-- Model 228I. Time histories of landings. Center of gravity, 34 percent M.A.C.

Figure 18.-- Model 228I. Number of skips and maximum and minimum trim and rise during landing. Center of gravity, 34 percent M.A.C.

Figure 19.-- Model 228C-1. Variation of trim with speed. Gross load, 123.5 pounds; acceleration 1.0  $\text{fps}^2$ .

(a) Flap deflection,  $0^\circ$ .

Figure 19.-- Continued.

(a) Flap deflection,  $0^\circ$ .

Figure 19.-- Continued.

(b) Flap deflection,  $20^\circ$ .

Figure 19.-- Continued.

(b) Flap deflection,  $20^\circ$ .

Figure 19.-- Continued.

(c) Flap deflection,  $40^\circ$ .

Figure 19.-- Concluded.

(c) Flap deflection,  $40^\circ$ .

Figure 20.-- Model 228C-1. Effect of flap deflection on the take-off stability. Gross load, 123.5 pounds; acceleration, 1.0  $\text{fps}^2$ .

Figure 21.-- Model 228C-1. Variation of trim with speed at three gross loads,  $\delta_f = 20^\circ$ , acceleration, 1.0  $\text{fps}^2$ .

Figure 22.-- Model 228C-1. Effect of gross load on the take-off stability.  $\delta_f = 20^\circ$ ; acceleration, 1.0  $\text{fps}^2$ .

Figure 23.-- Model 228C-1. Variation of trim with speed at two accelerations. Gross load, 123.5 pounds;  $\delta_f = 20^\circ$ .

Figure 24.-- Model 228C-1. Effect of acceleration on the take-off stability. Gross load, 123.5 pounds;  $\delta_f = 20^\circ$ .

## FIGURE LEGENDS - Continued

Figure 25.- Model 228D-1. Take-off stability. Gross load, 123.5 pounds;  $\delta_f = 20^\circ$ ; acceleration, 1.0 fps<sup>2</sup>.

Figure 26.- Model 228H. Take-off stability. Gross load, 123.5 pounds;  $\delta_f = 20^\circ$ ; acceleration, 1.0 fps<sup>2</sup>.

Figure 27.- Model 228G-1. Take-off stability. Gross load 123.5 pounds;  $\delta_f = 20^\circ$ ; acceleration, 1.0 fps<sup>2</sup>.

Figure 28.- Model 228J-1. Take-off stability. Gross load, 123.5 pounds;  $\delta_f = 20^\circ$ ; acceleration, 1.0 fps<sup>2</sup>.

Figure 29.- Model 228C-1, 228G-1 and 228J-1. Effect of angle of after-body keel on the take-off stability. Gross load, 123.5 pounds;  $\delta_f = 20^\circ$ ; acceleration, 1.0 fps<sup>2</sup>.

Figure 30.- Model 228I. Take-off stability. Gross load, 123.5 pounds;  $\delta_f = 20^\circ$ ; acceleration, 1.0 fps<sup>2</sup>.

Figure 31.- Model 228C-1. Variation of excess thrust and trim with speed.  $\delta_f = 20^\circ$ ; center of gravity, 30 percent mean aerodynamic chord; take-off power.

Figure 32.- Model 228J-1. Bow spray photographs. Flap deflection,  $20^\circ$ ; elevator deflections,  $0^\circ$ ; center of gravity, 34-percent mean aerodynamic chord; take-off power; gross load, 123.5 pounds.

Figure 32.- Model 228J-1, continued.

Figure 32.- Model 228J-1, continued.

Figure 32.- Model 228J-1, concluded.

Figure 33.- Model 228D-1. Speed range over which spray strikes the propellers and the flaps. Flap deflection,  $20^\circ$ ; elevator deflection  $0^\circ$ ; center of gravity, 30-percent mean aerodynamic chord; take-off power.

Figure 34.- Model 228 C-1. Spray over tail turret near hump speed. Flap deflection,  $20^\circ$ ; center of gravity. 30-percent mean aerodynamic chord; take-off power; gross load, 123.5 pounds.

FIGURE LEGENDS -- Concluded

Figure 35.-- Model 228 C-1. Effect of power on spray over tail assembly at speeds near hump. Flap deflection,  $20^{\circ}$ ; center of gravity, 30-percent mean aerodynamic chord; gross load, 123.5 pounds.

Figure 36.-- Model 228 C-1. Spray on tail near upper trim limit of stability. Flap deflection,  $0^{\circ}$ ; center of gravity, 34-percent mean aerodynamic chord; take-off power; gross load, 123.5 pounds.

251

NACA RM No. L7E28

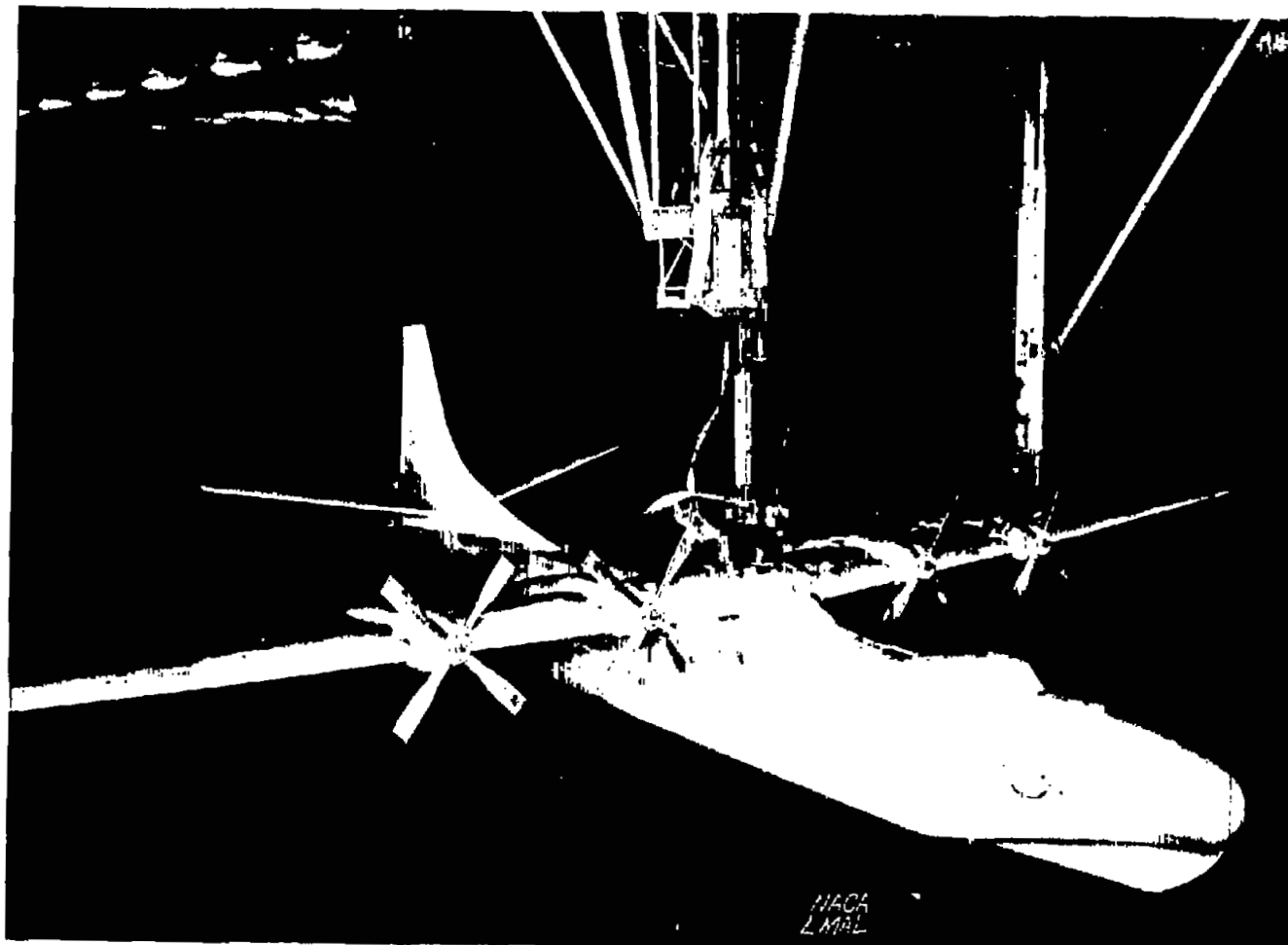
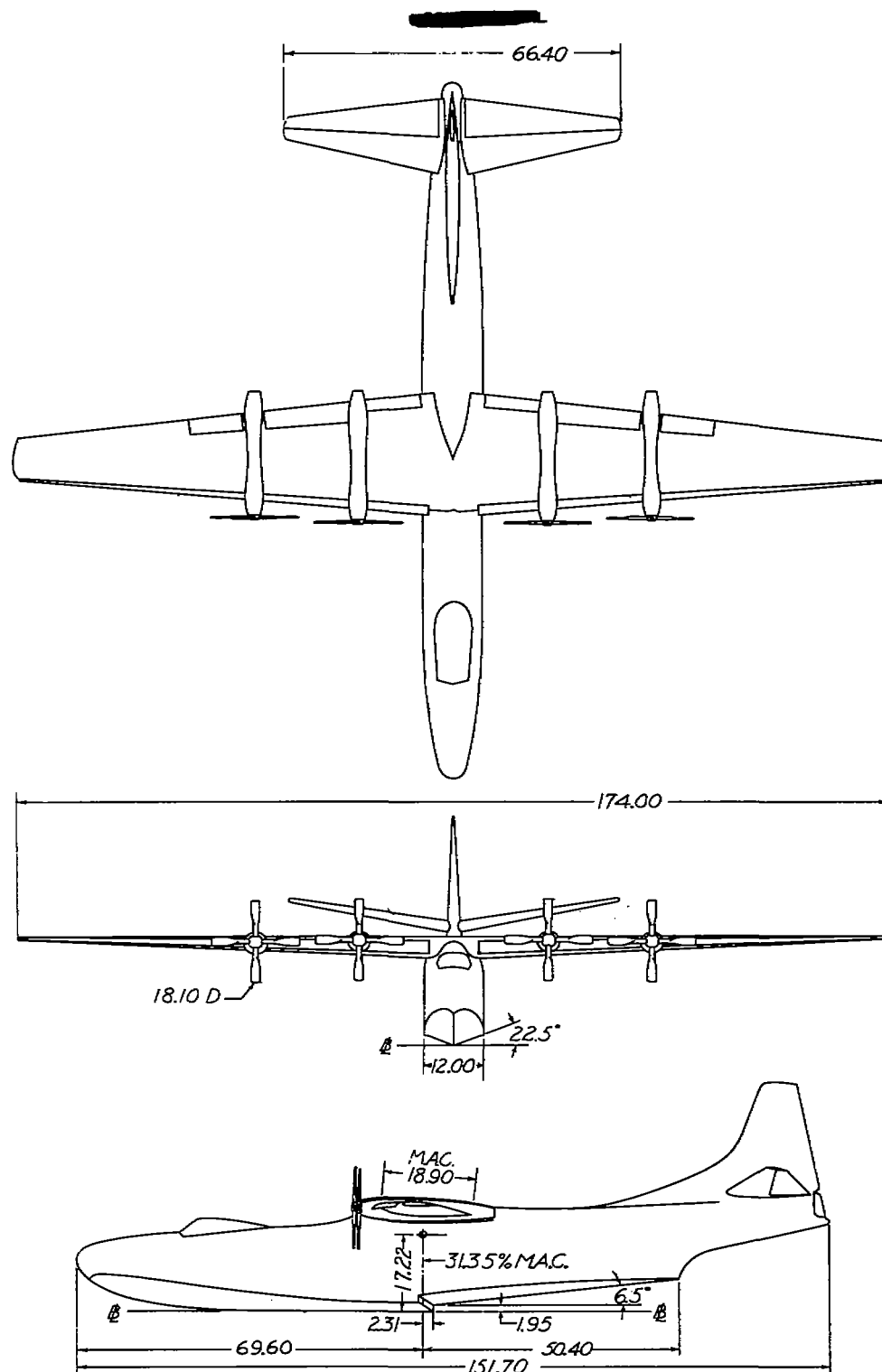


Figure 1.- Model 228C-1 on towing apparatus.

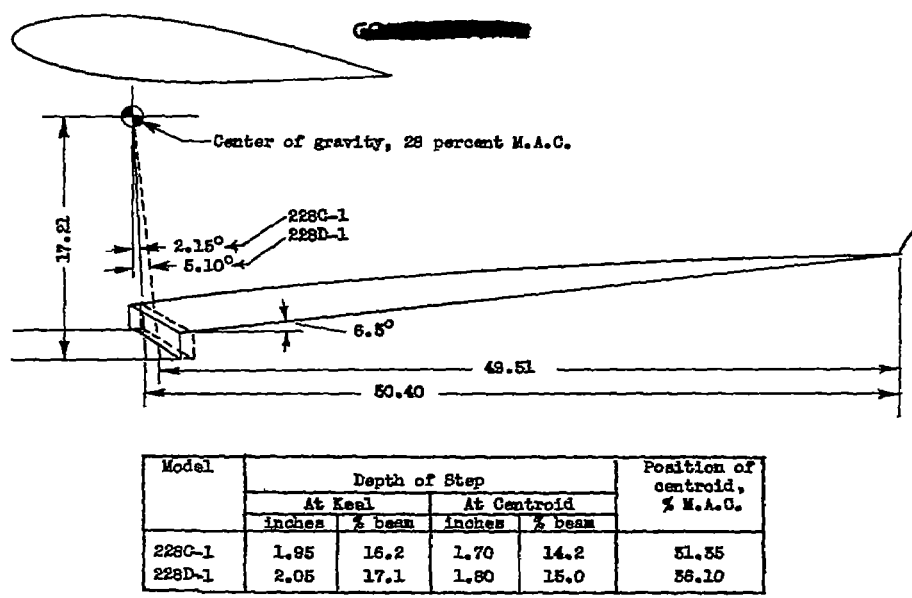
NATIONAL ADVISORY COMMITTEE FOR AERONAUTICS  
LANGLEY MEMORIAL AERONAUTICAL LABORATORY - LANGLEY FIELD, VA

Fig. 1

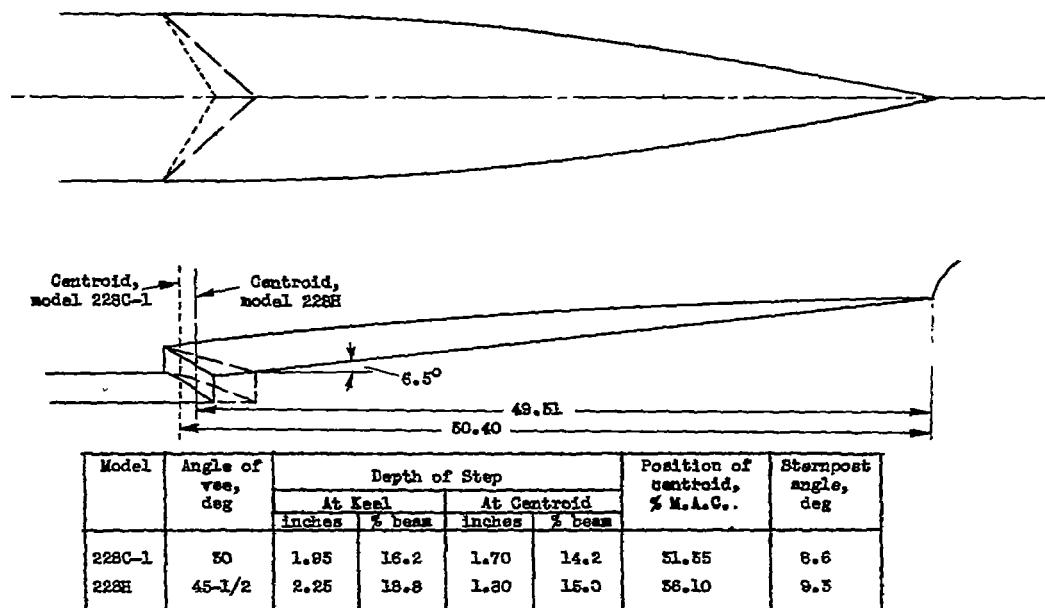


NATIONAL ADVISORY  
COMMITTEE FOR AERONAUTICS

FIGURE 2.- MODEL 228C-1. GENERAL ARRANGEMENT.  
(DIMENSIONS IN INCHES.)



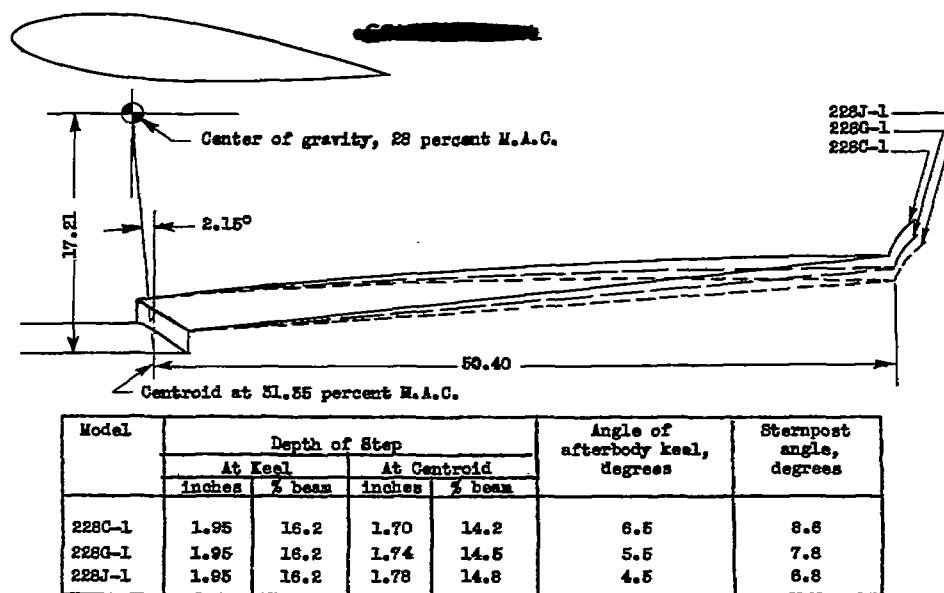
(a) Model 228D-1. Step moved aft.



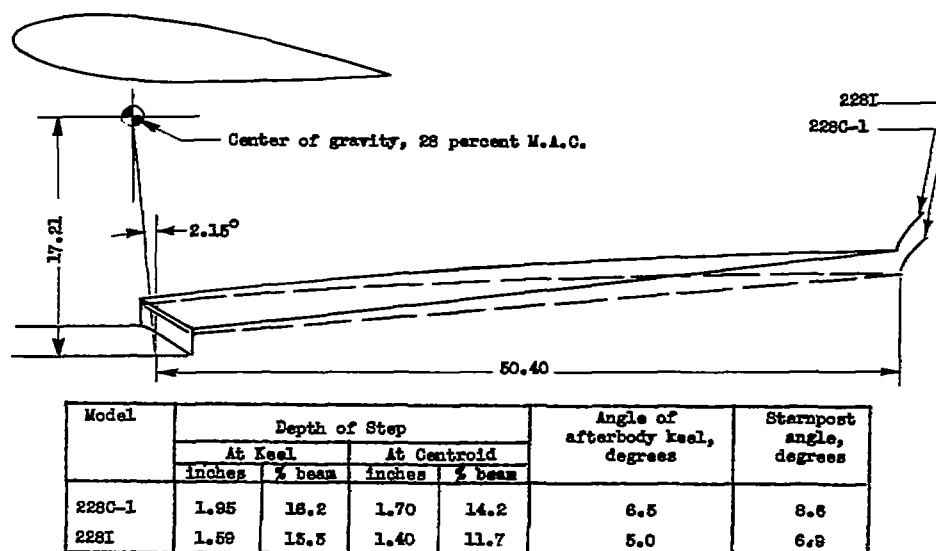
(b) Model 228H. 45 1/2° - vee planform of step.

NATIONAL ADVISORY  
COMMITTEE FOR AERONAUTICS

Figure 3.- Modifications to basic model 228C-1.

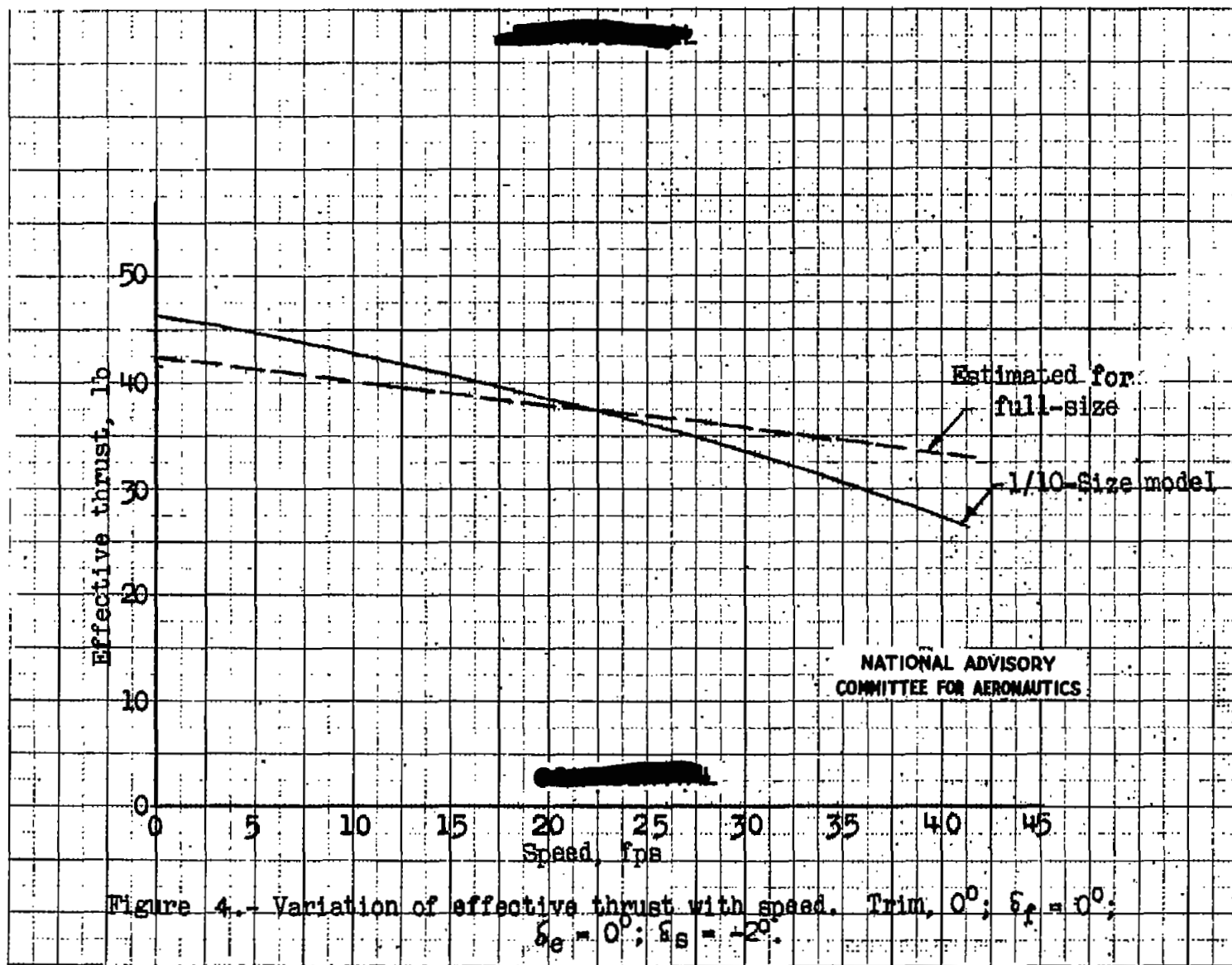


(c) Models 228G-1 and J-1. Angle of afterbody reduced.



(d) Model 228I. Depth of step and angle of afterbody keel reduced.

Figure 3.- Concluded.



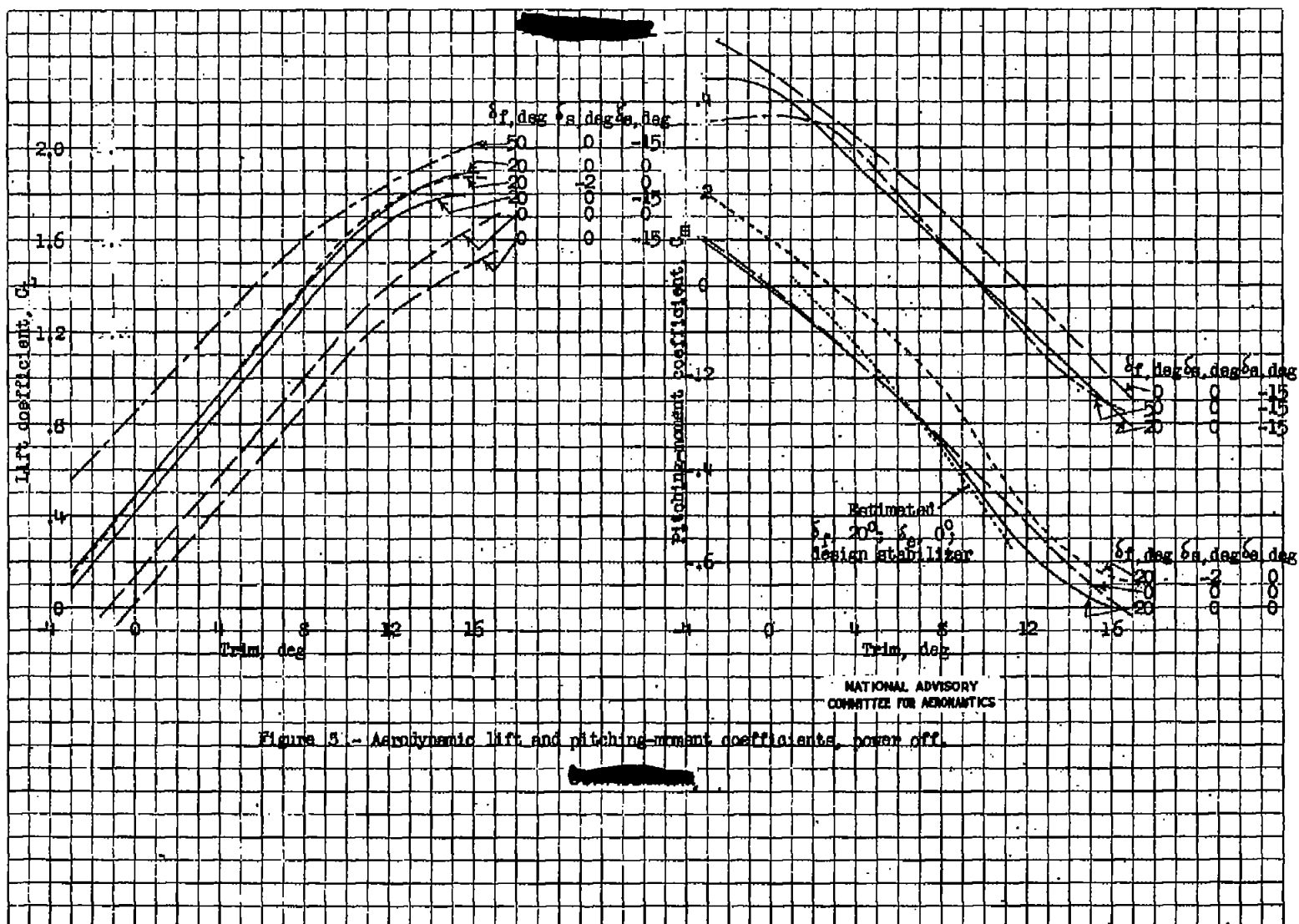


Figure 5. - Aerodynamic lift and pitching-moment coefficients, power off.

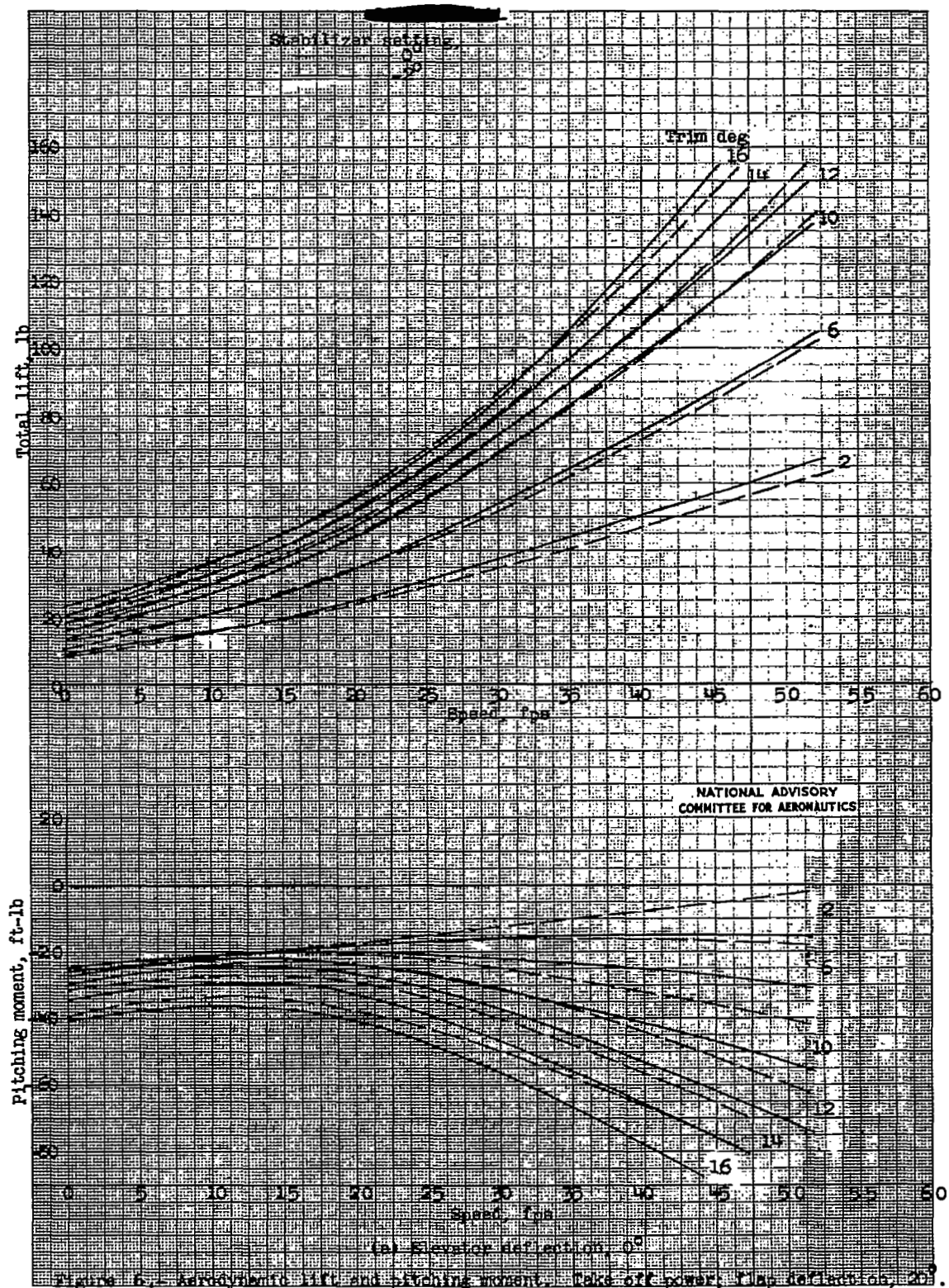
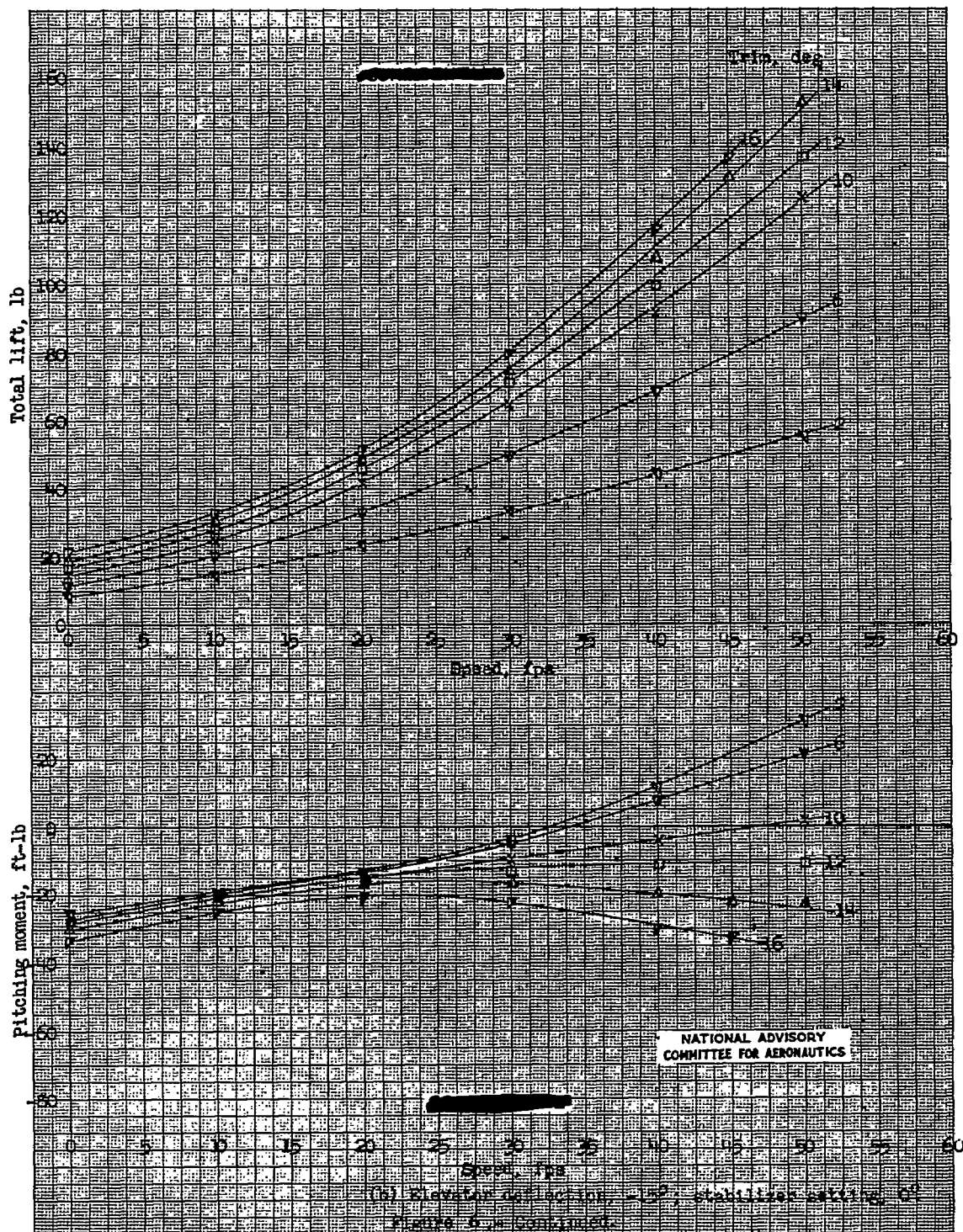
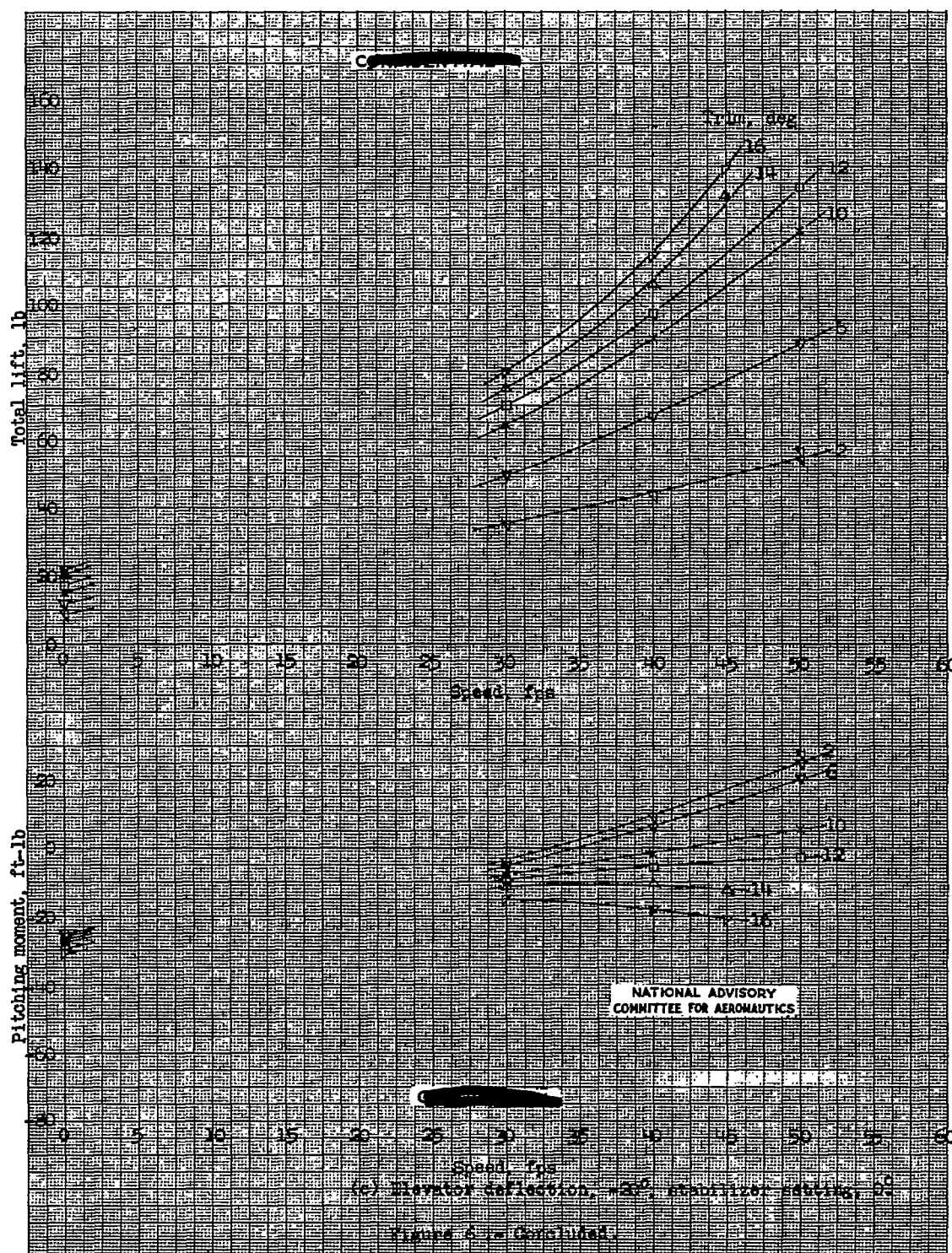
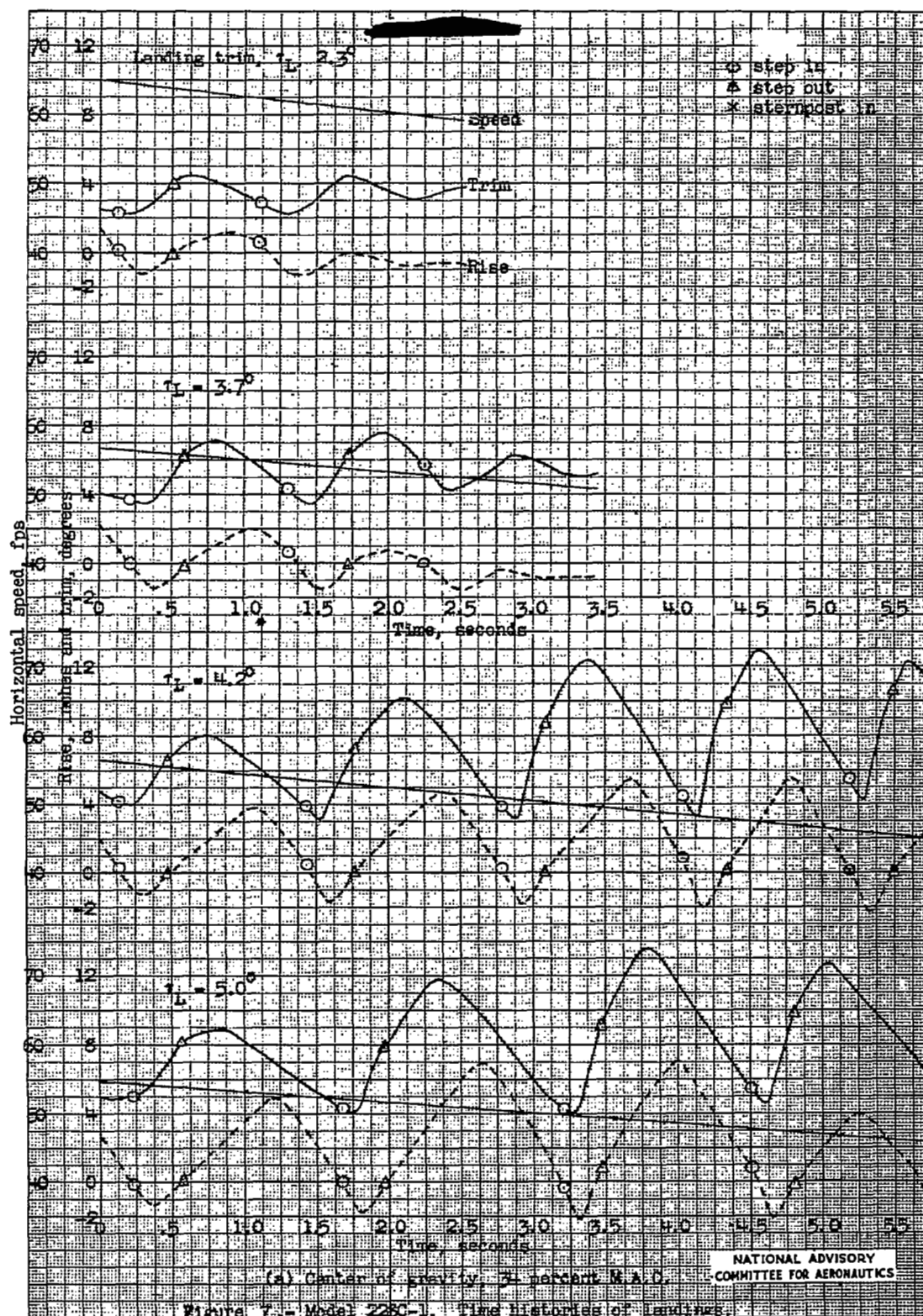
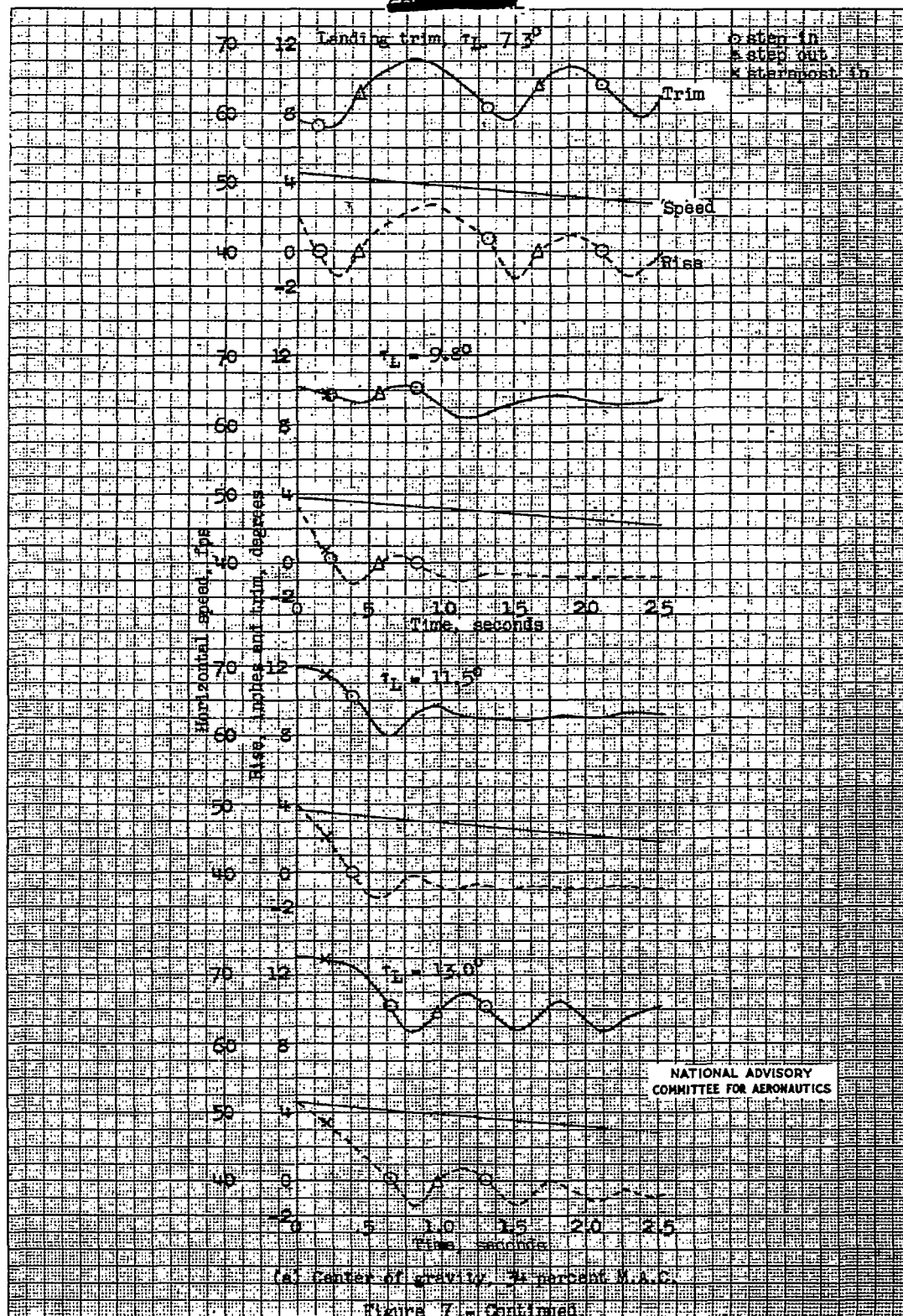


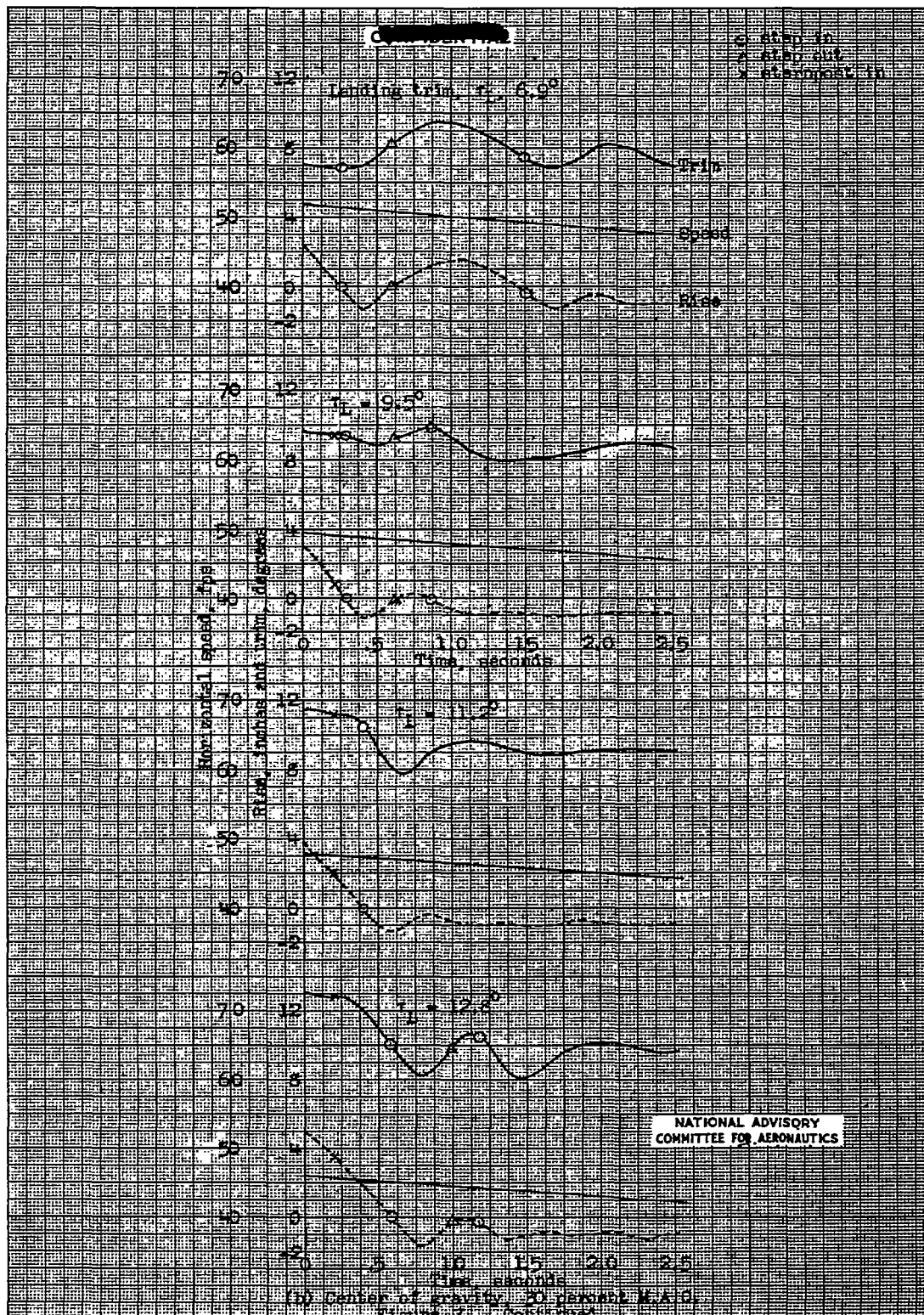
Figure 6a.—Aerodynamic lift and pitching moment. Take-off power. Flap deflection, 20°.

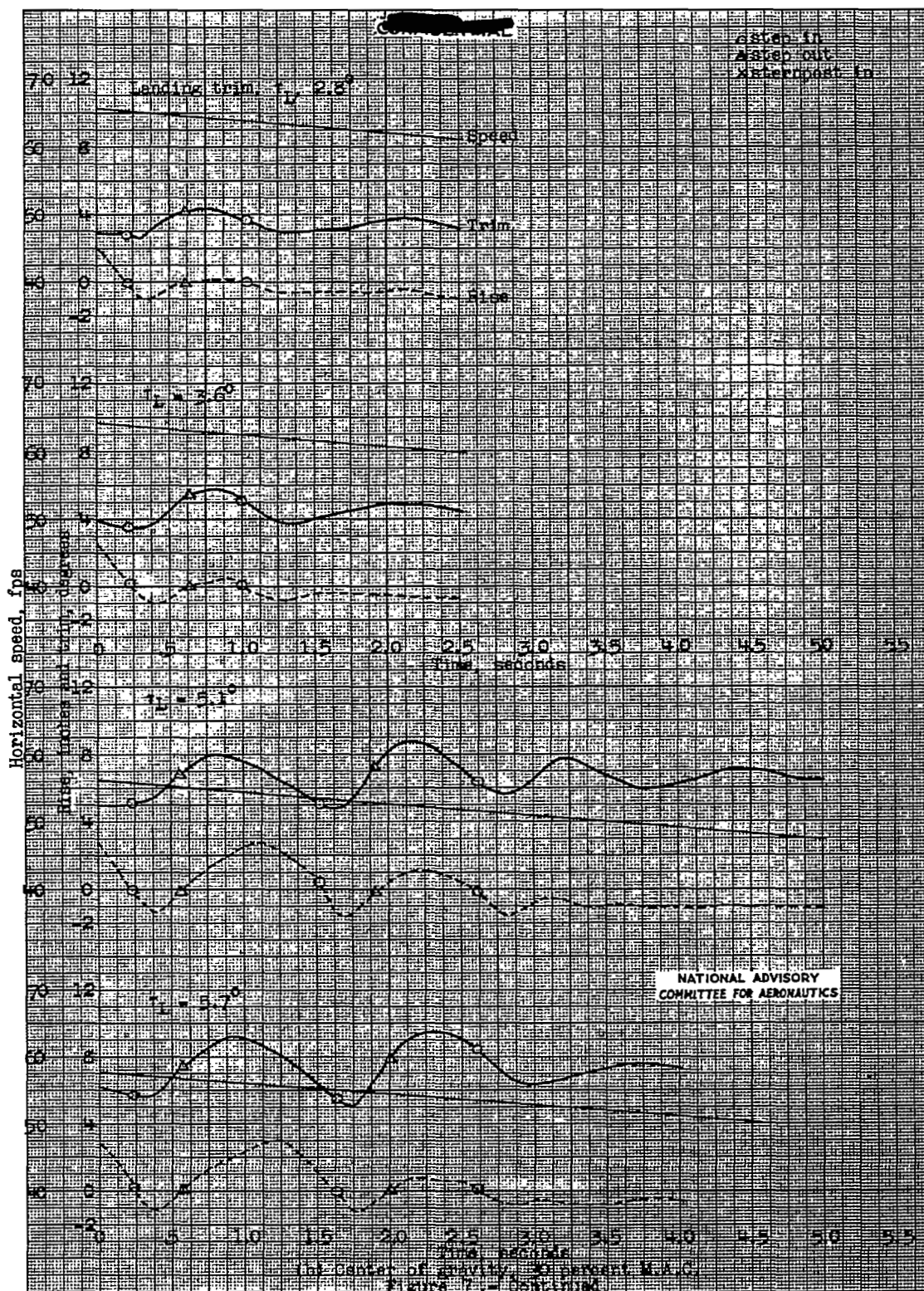


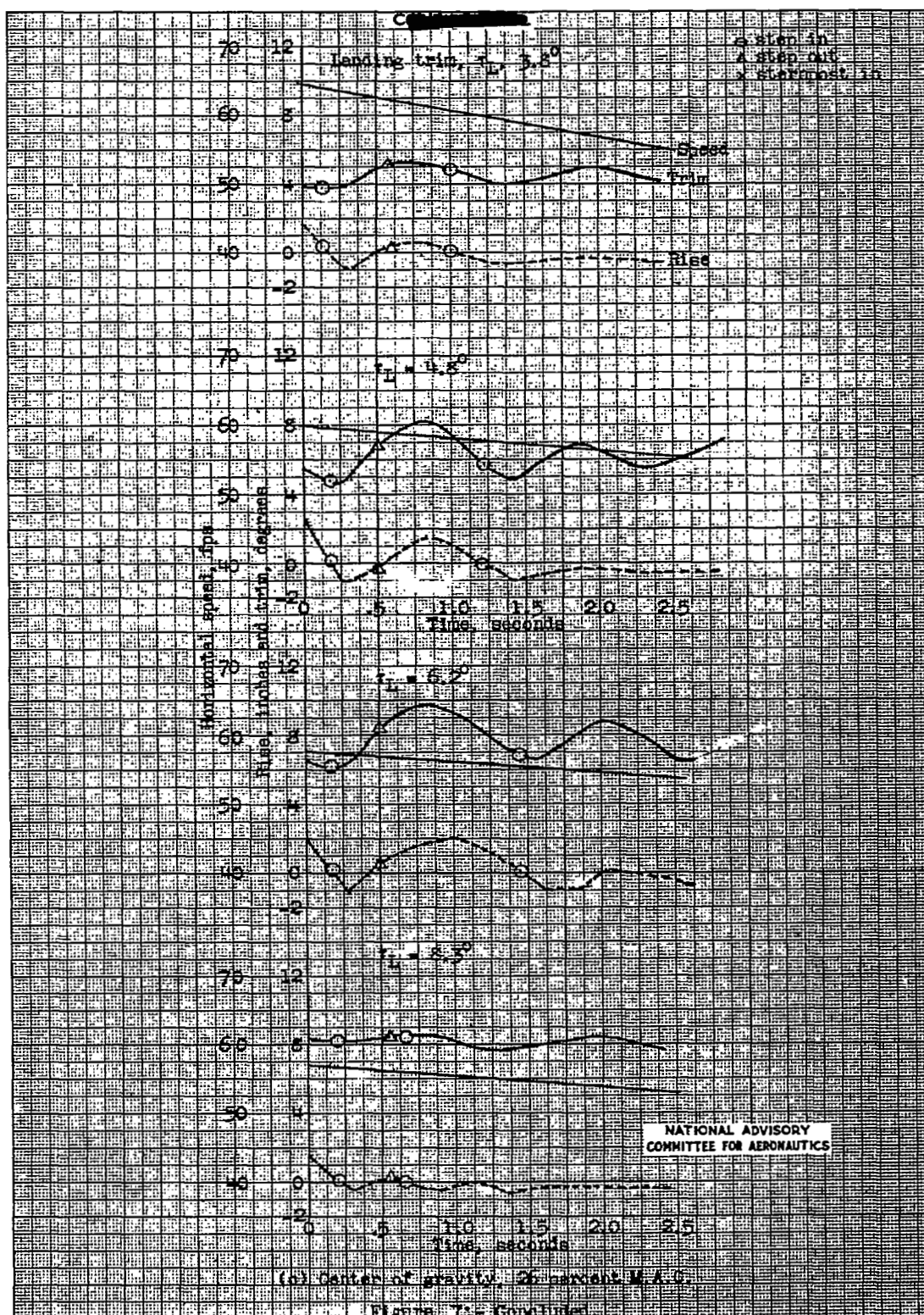












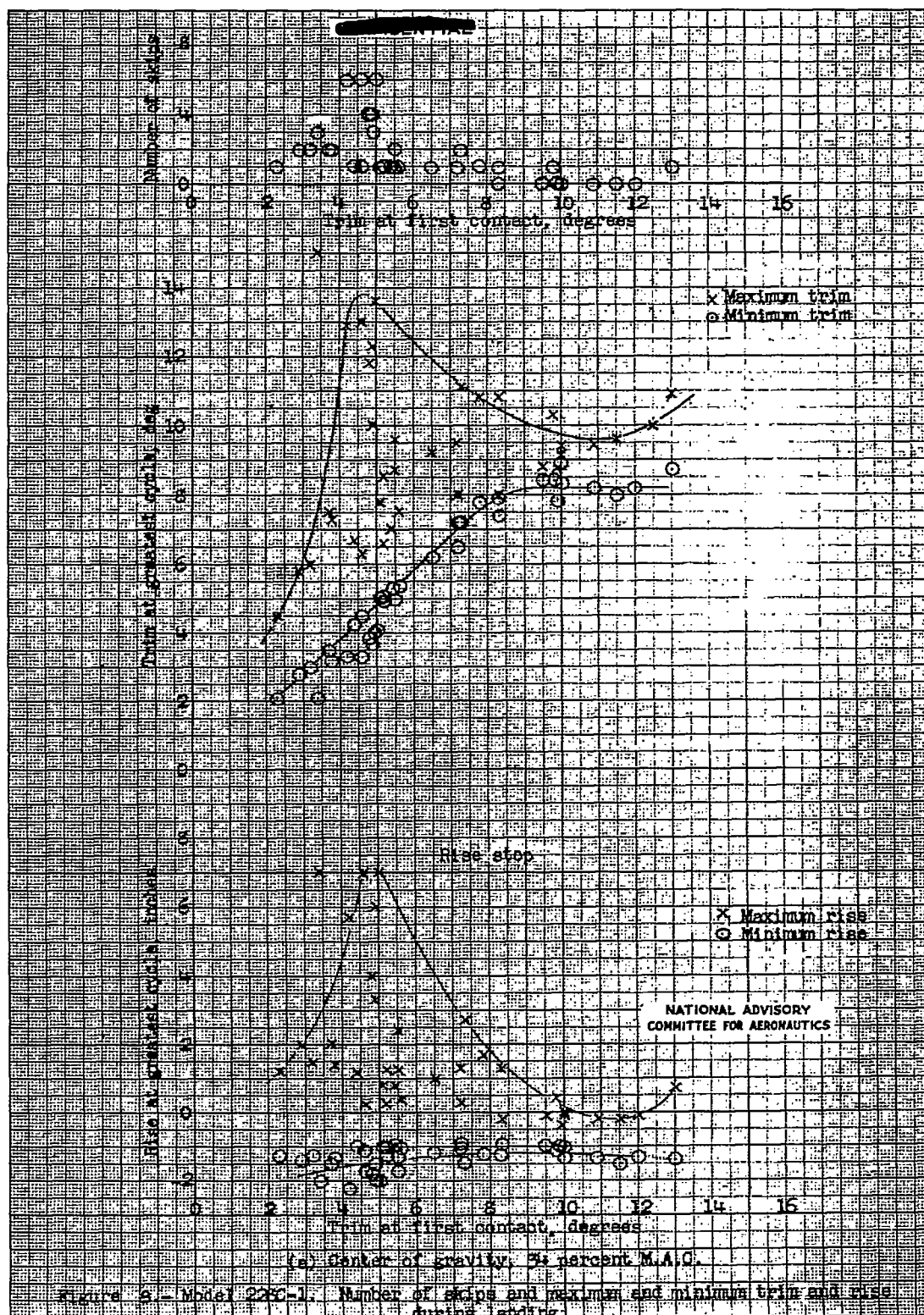
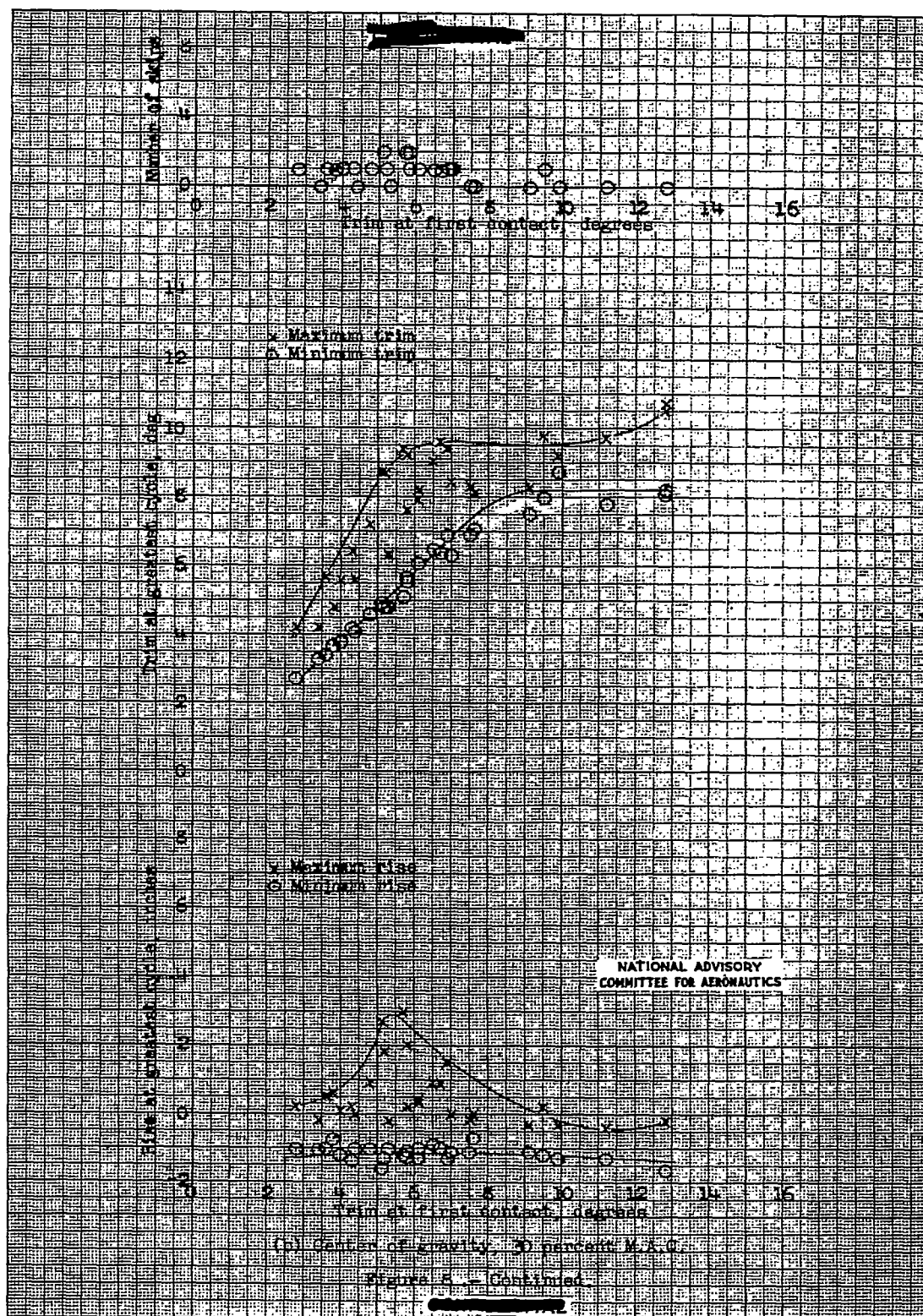
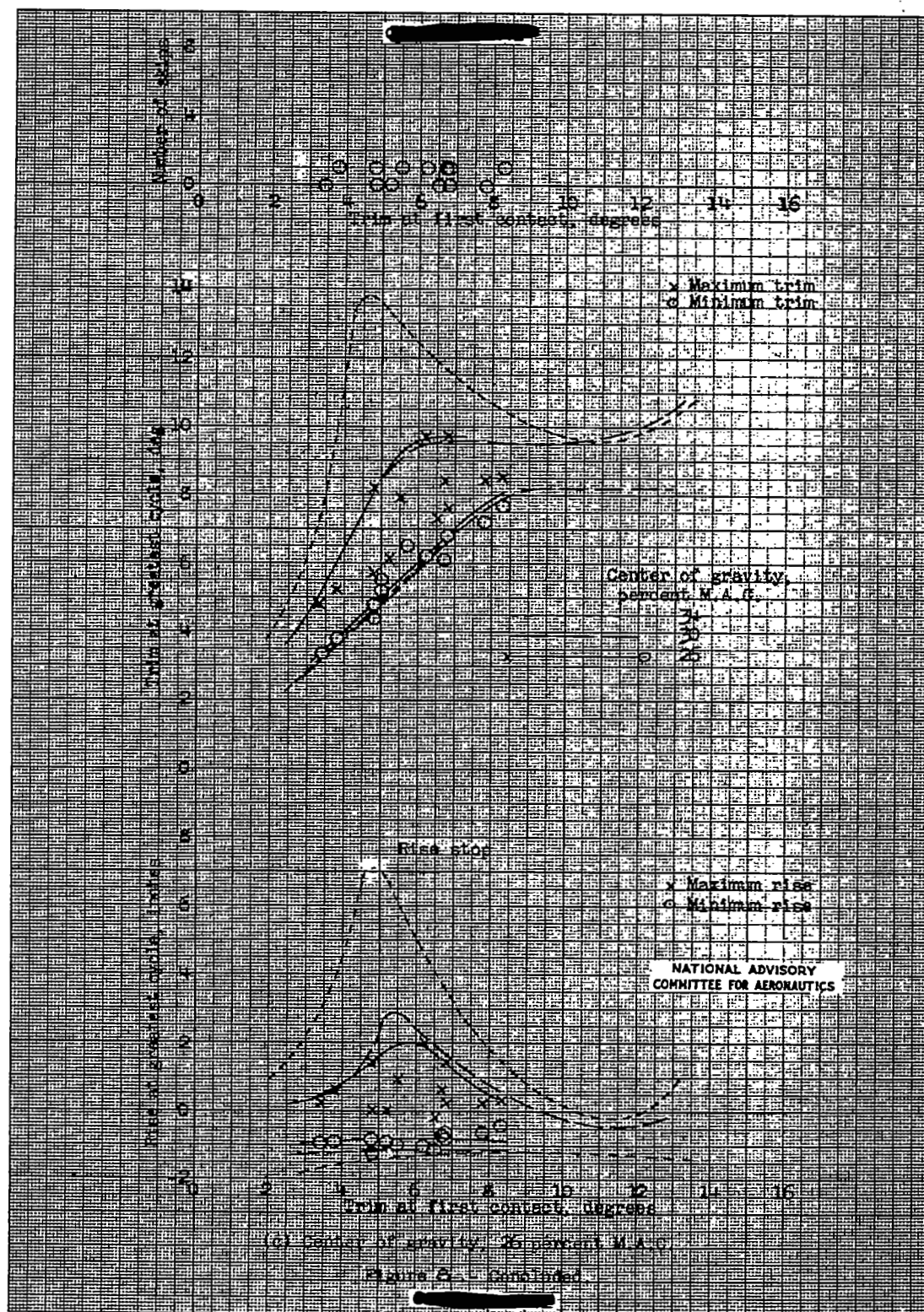
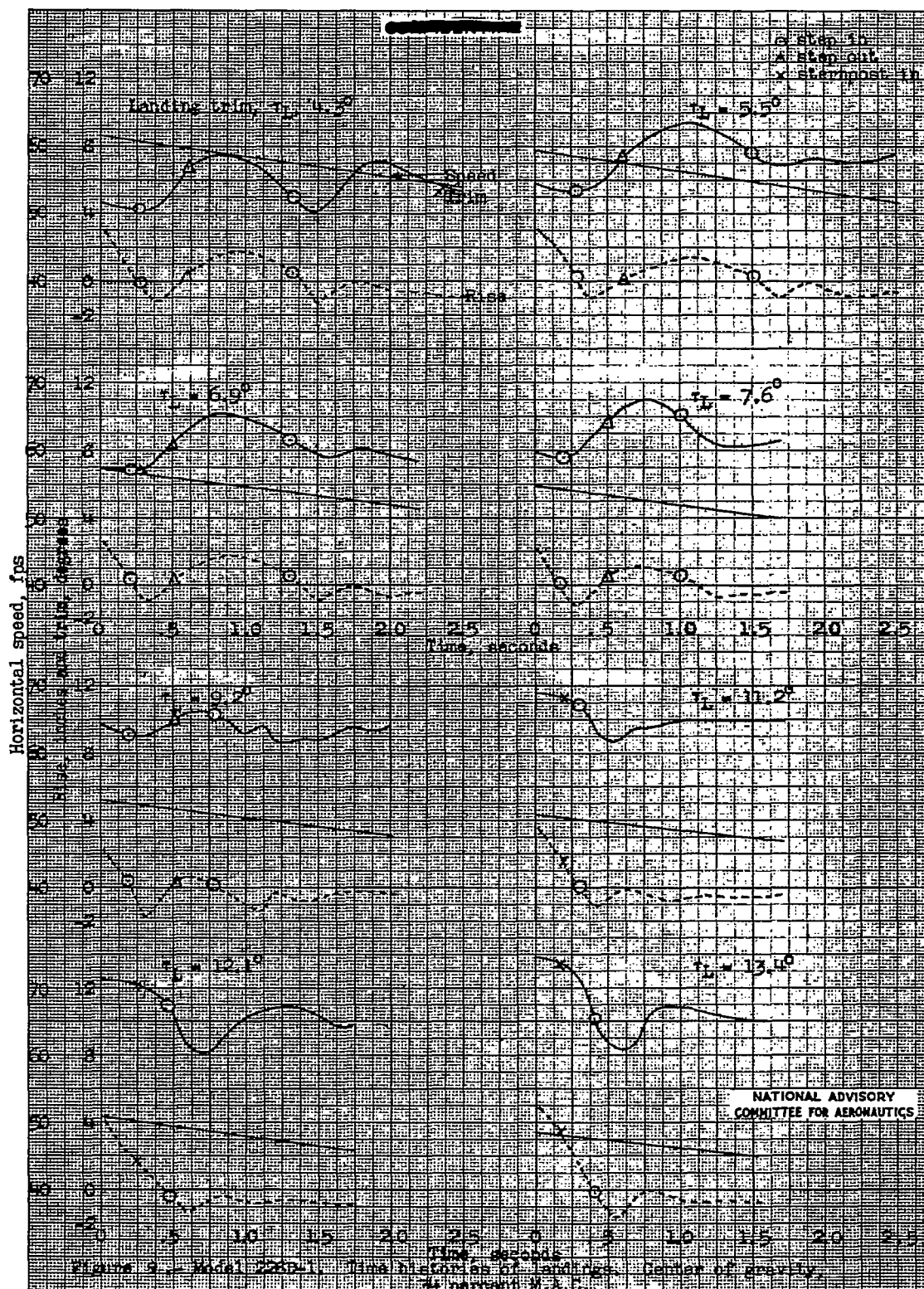
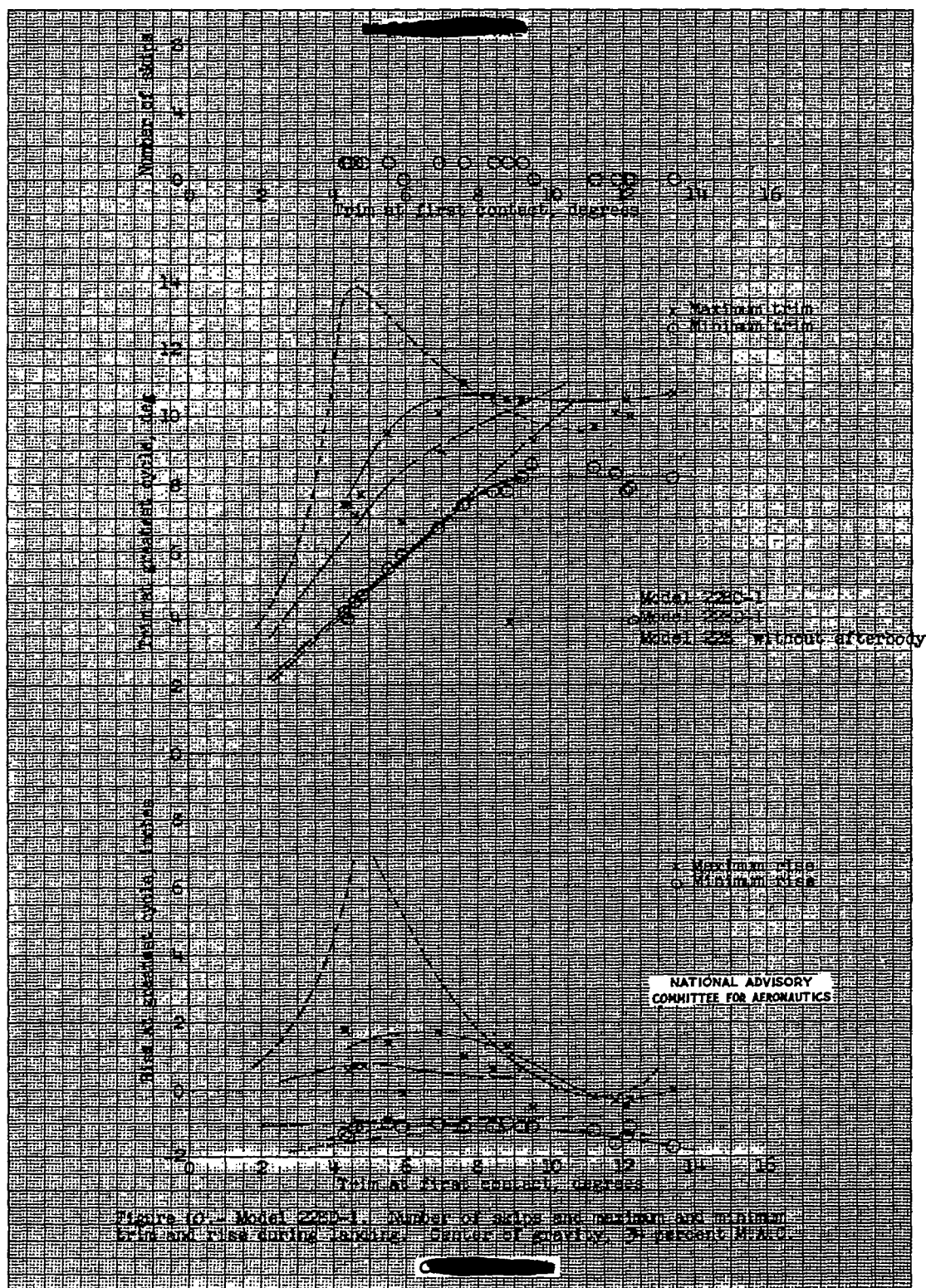


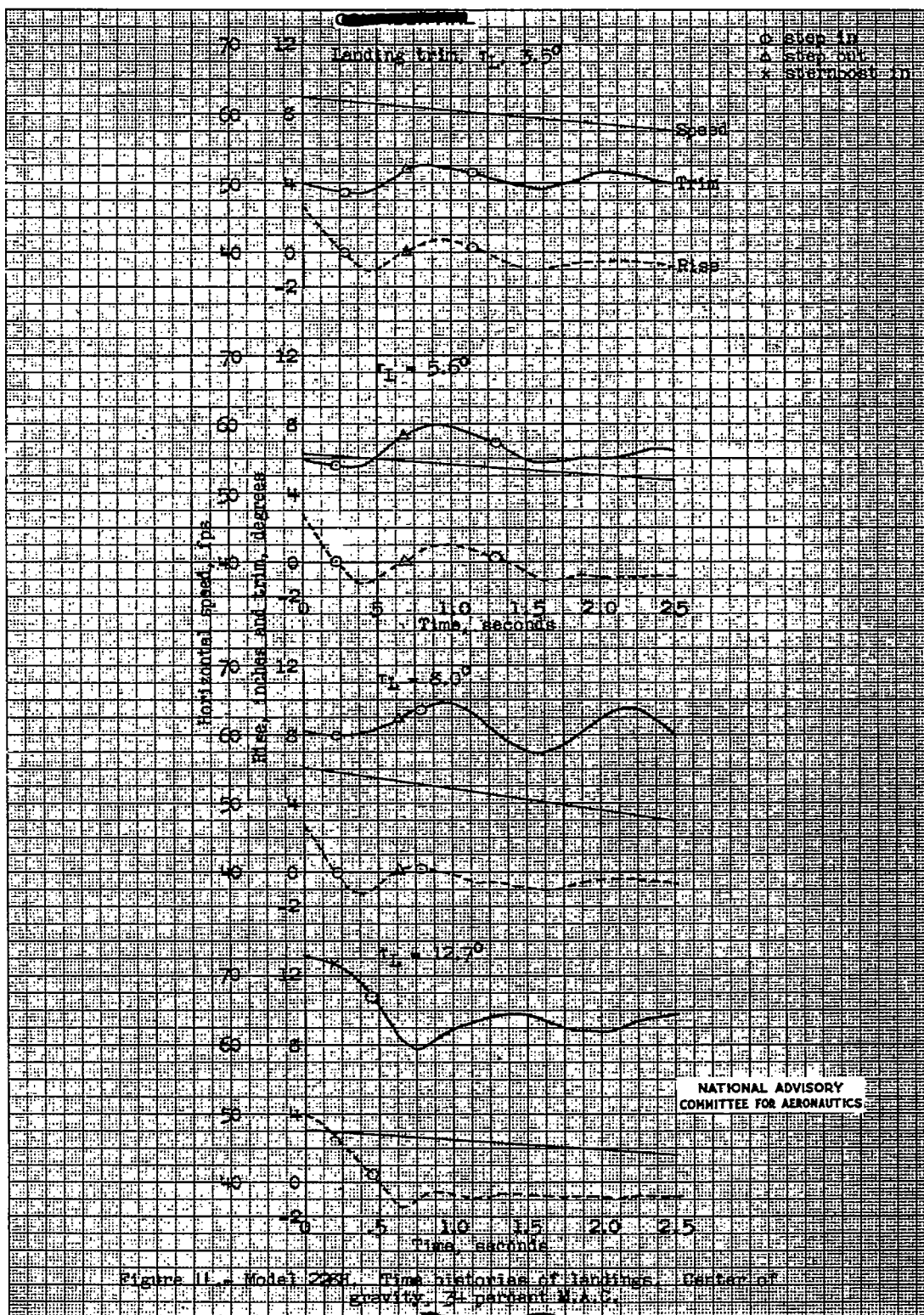
Figure 8.- Model 22C-1. Number of skips and maximum and minimum trim and rise during landing.

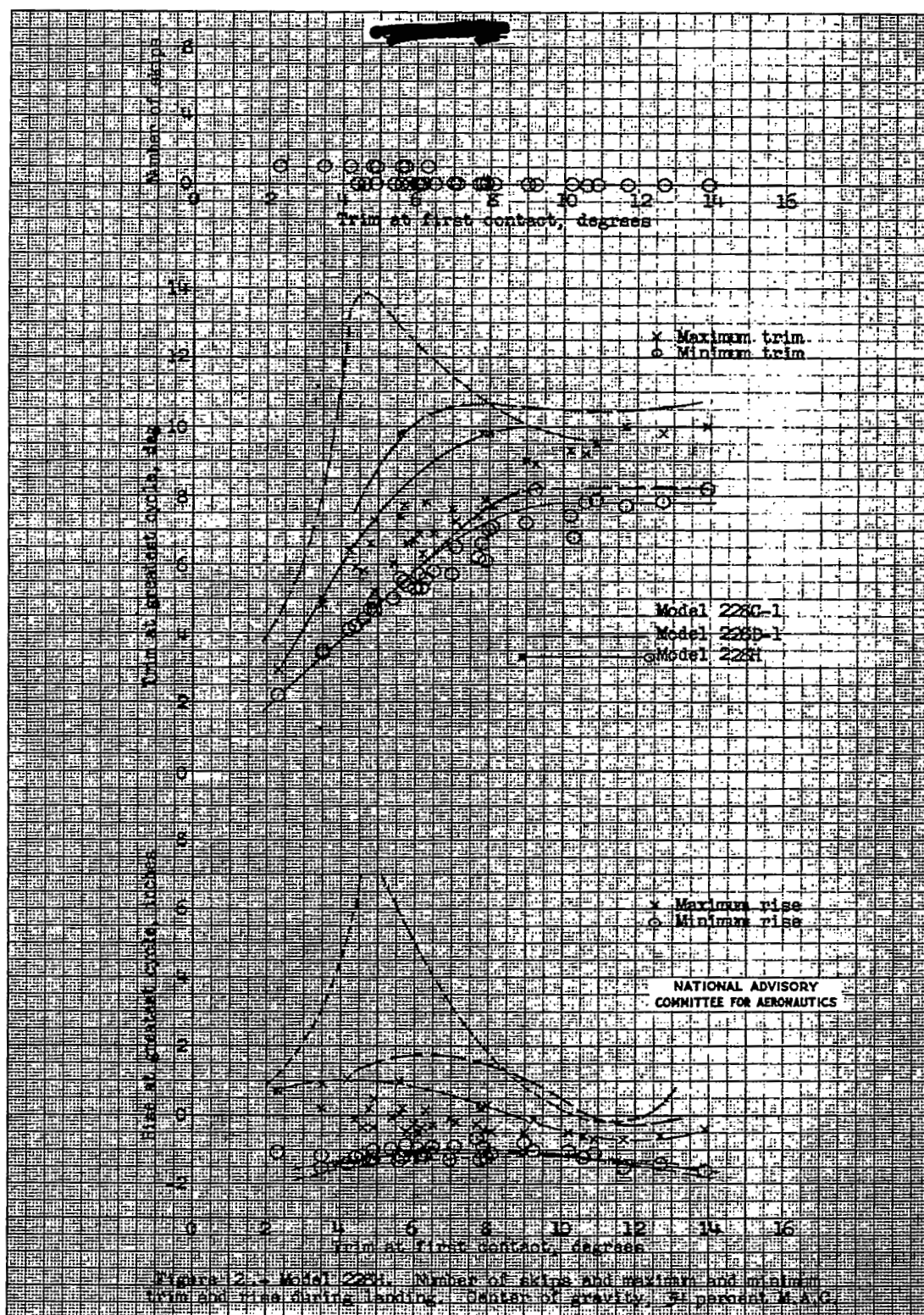












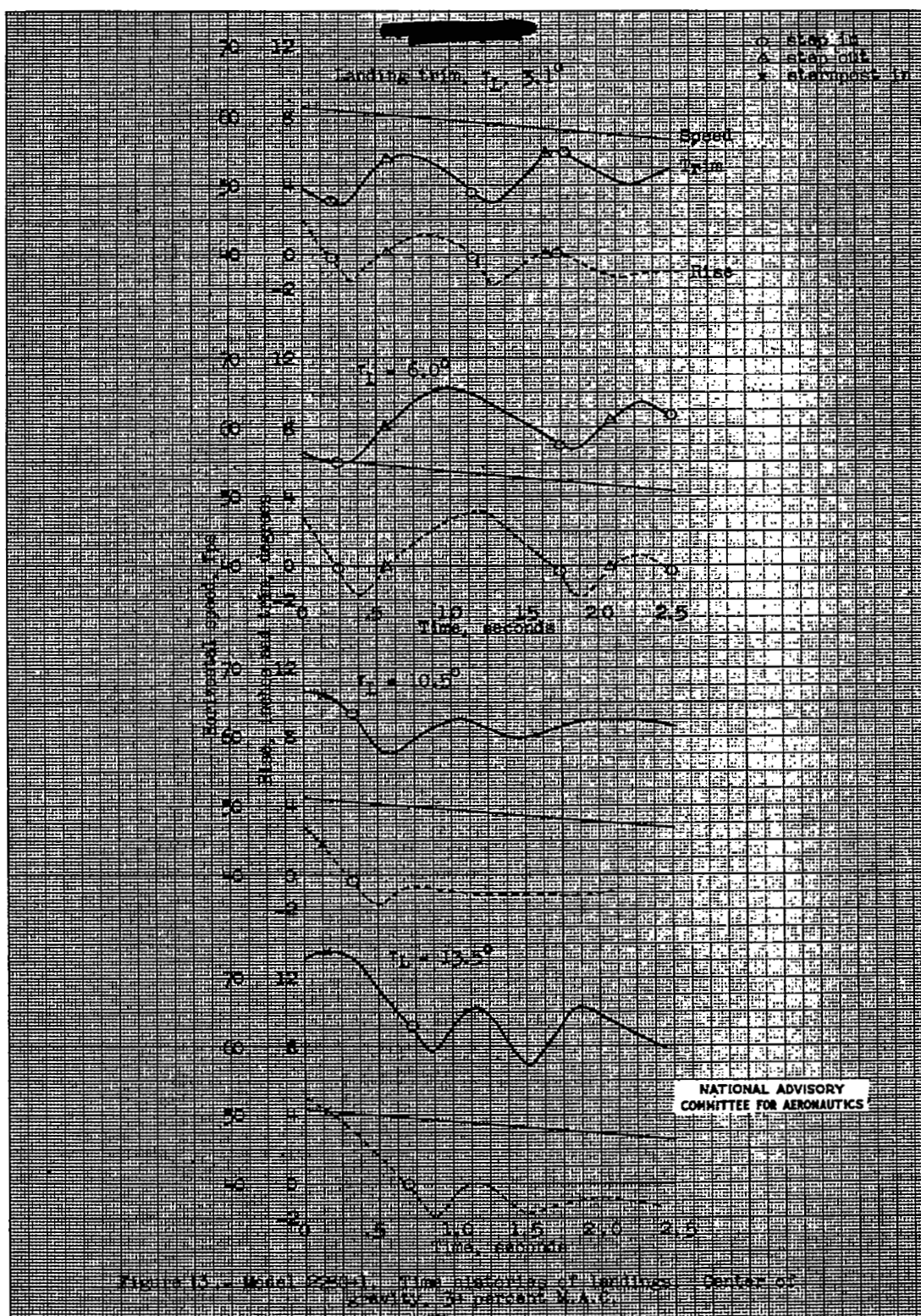


Figure 13 - Model 224a1. Time histories of landings. Center of gravity, 30 percent M.A.C.

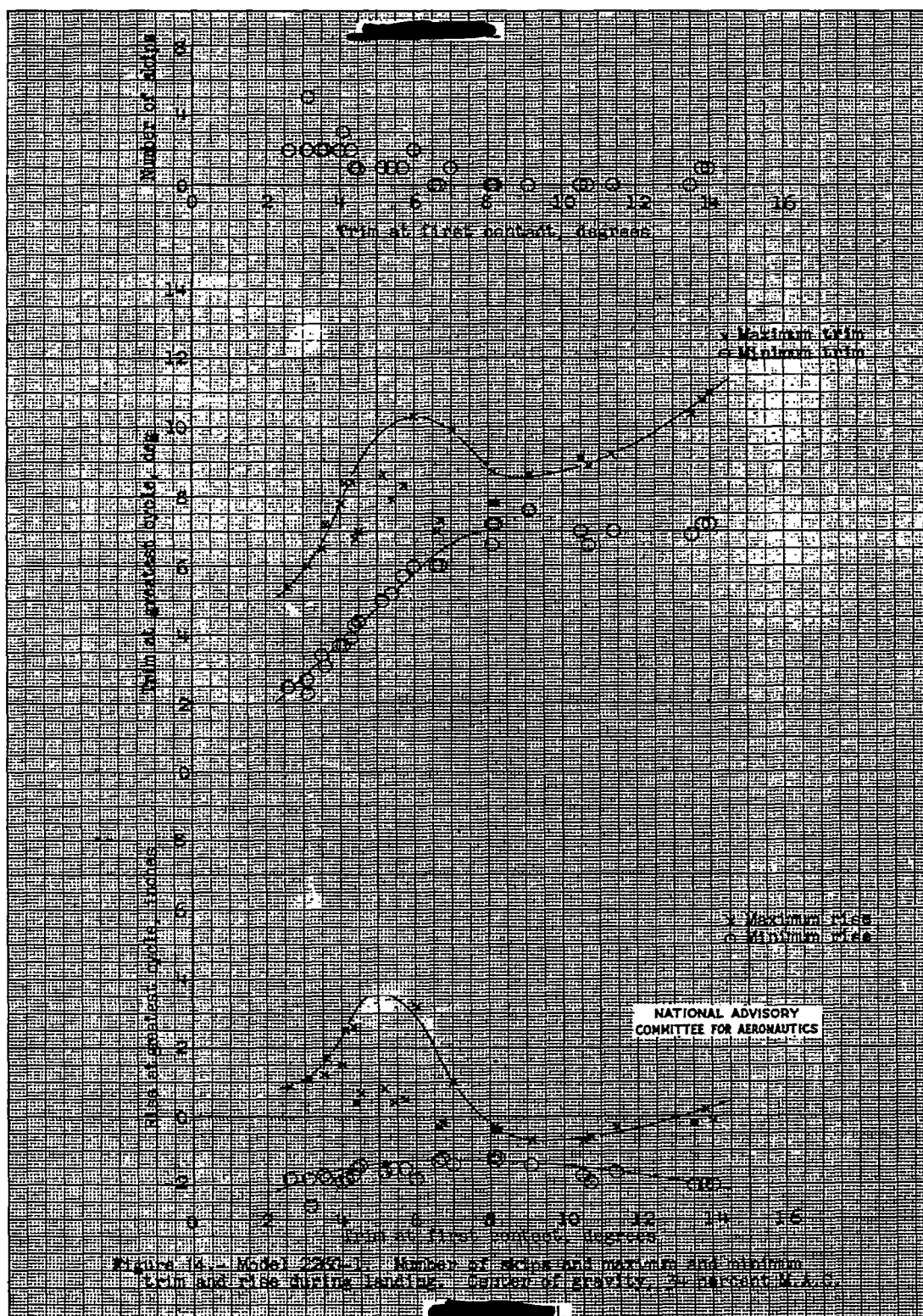
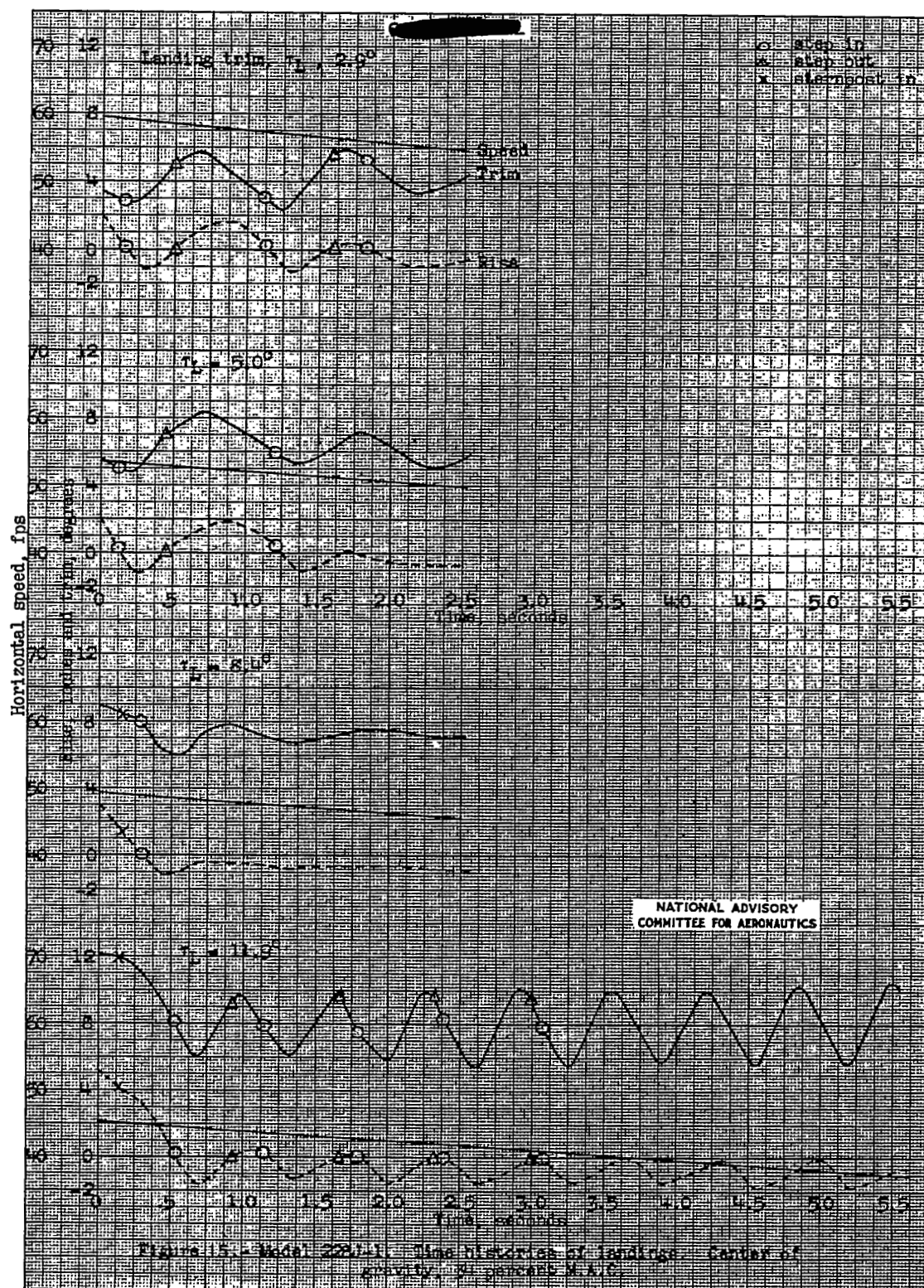
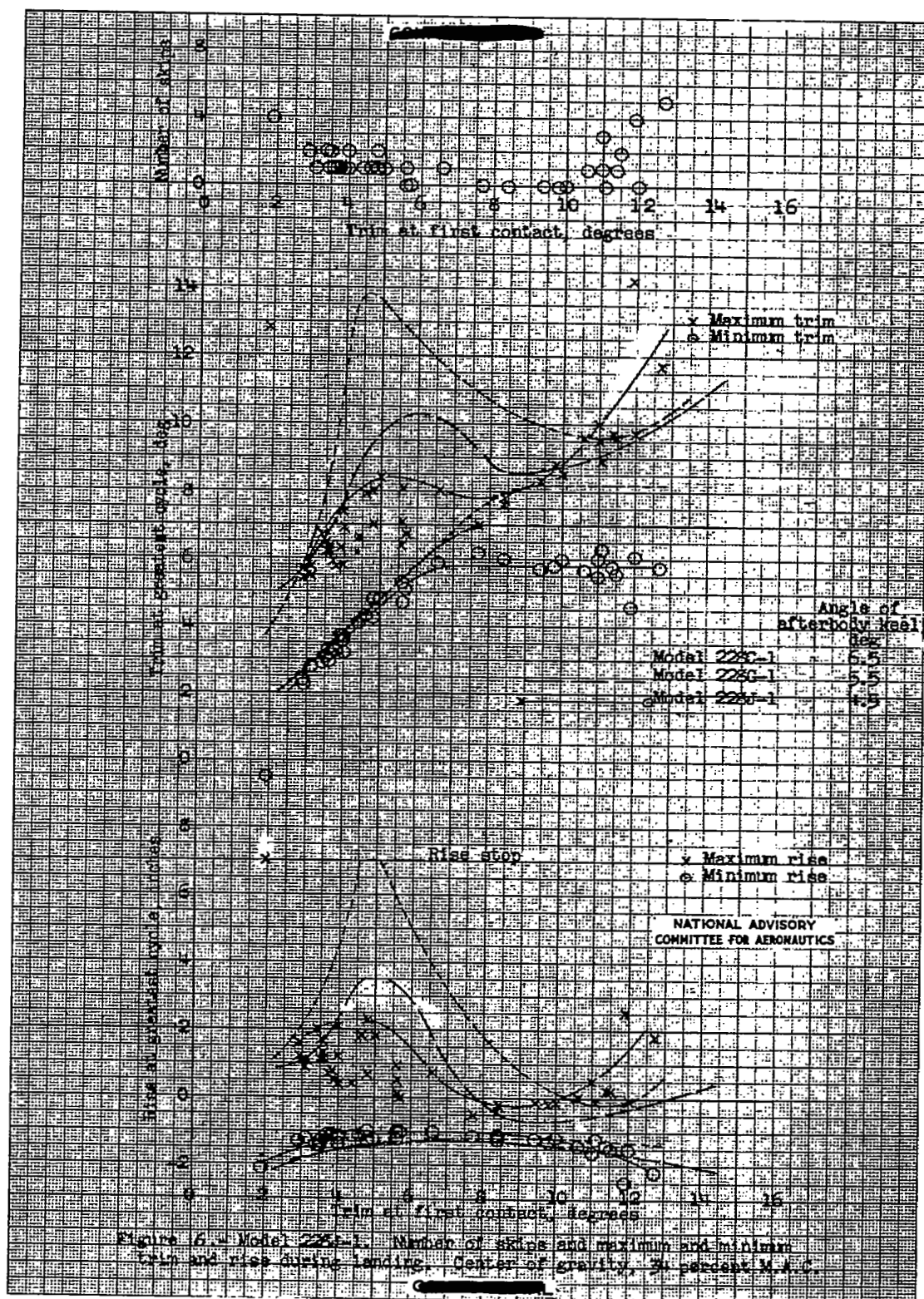
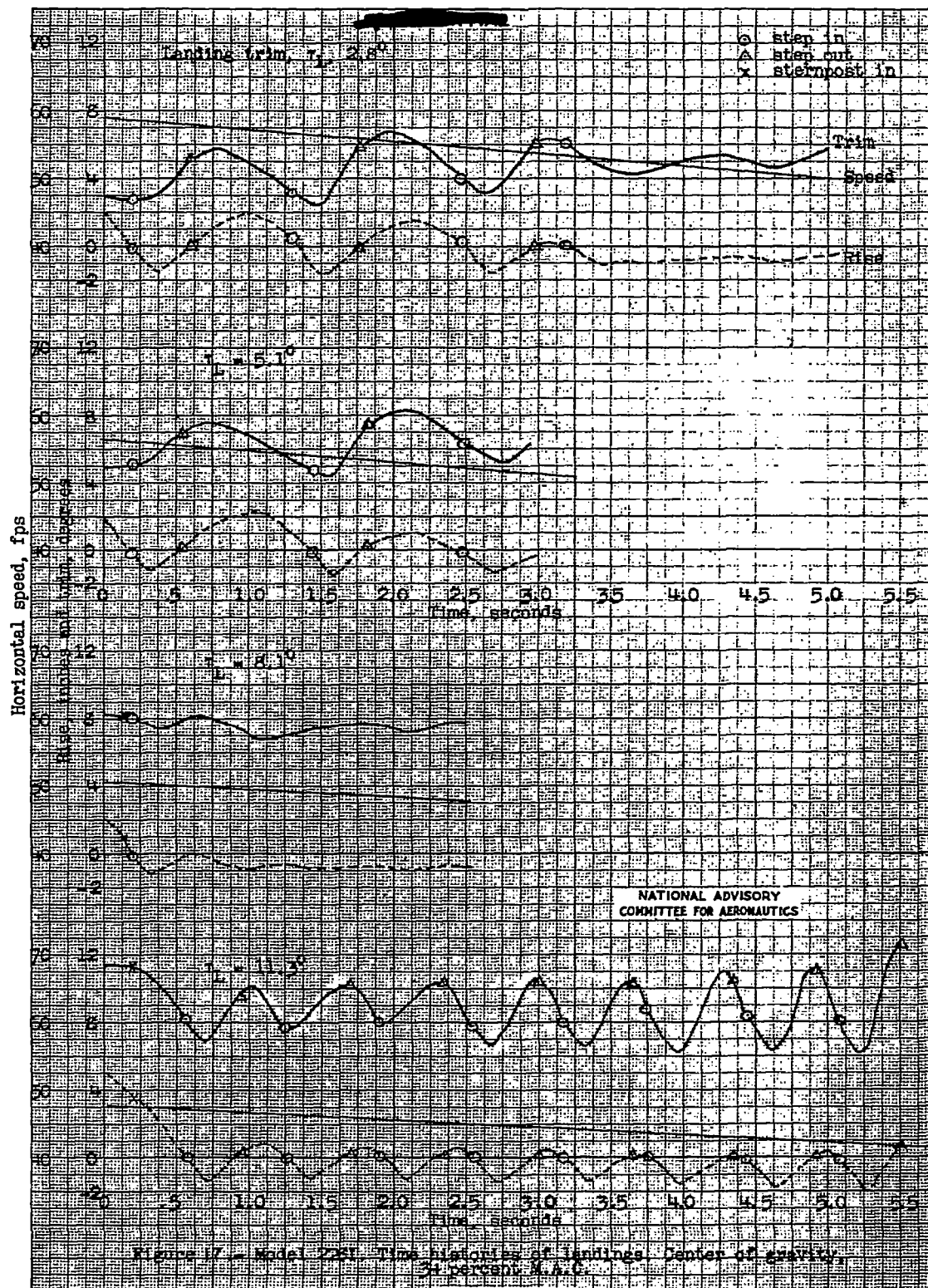
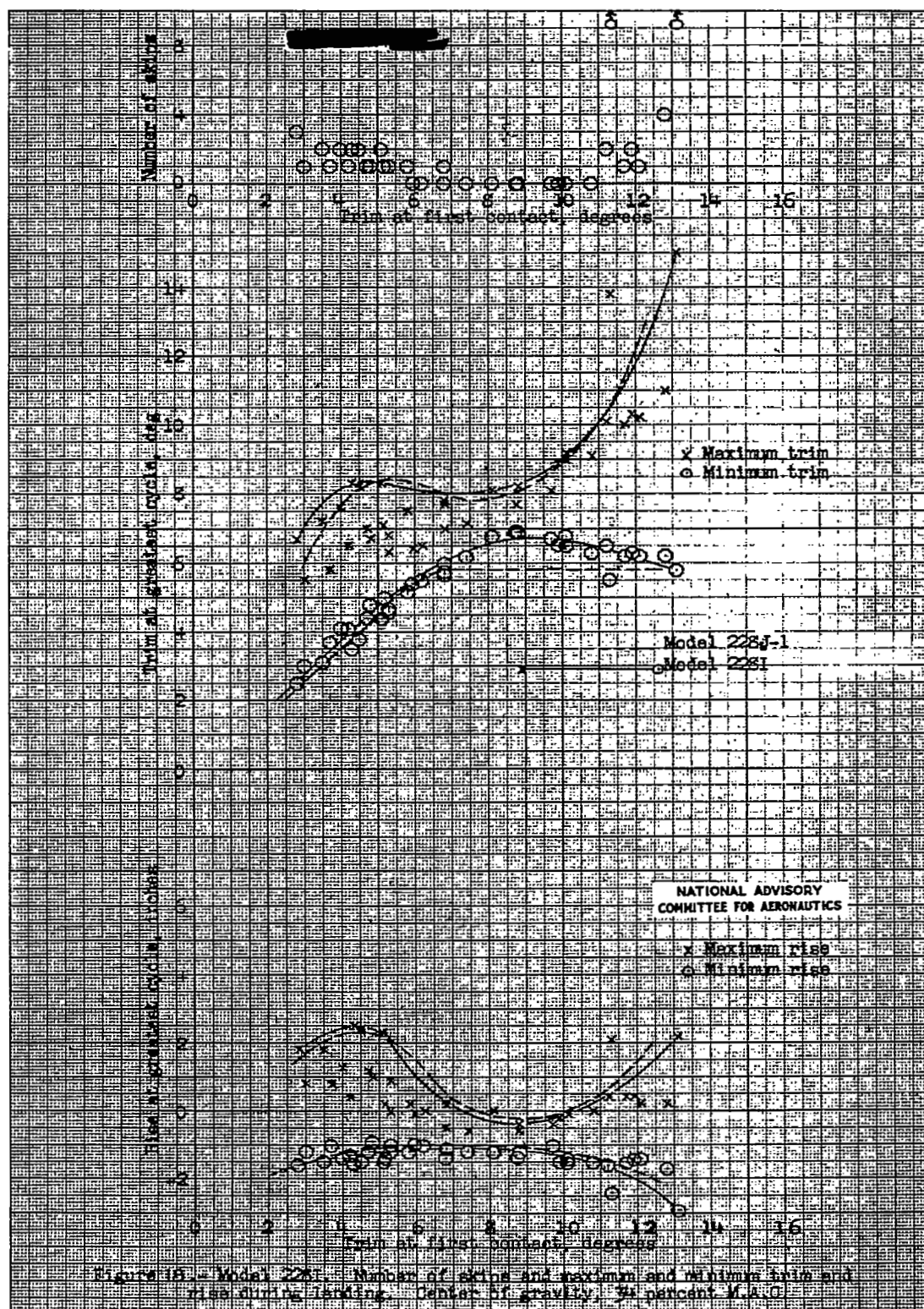


Figure 14. - Model 2280-1. Number of bounces and maximum and minimum trim and rise during landing. Center of gravity, 24 percent M.A.C.

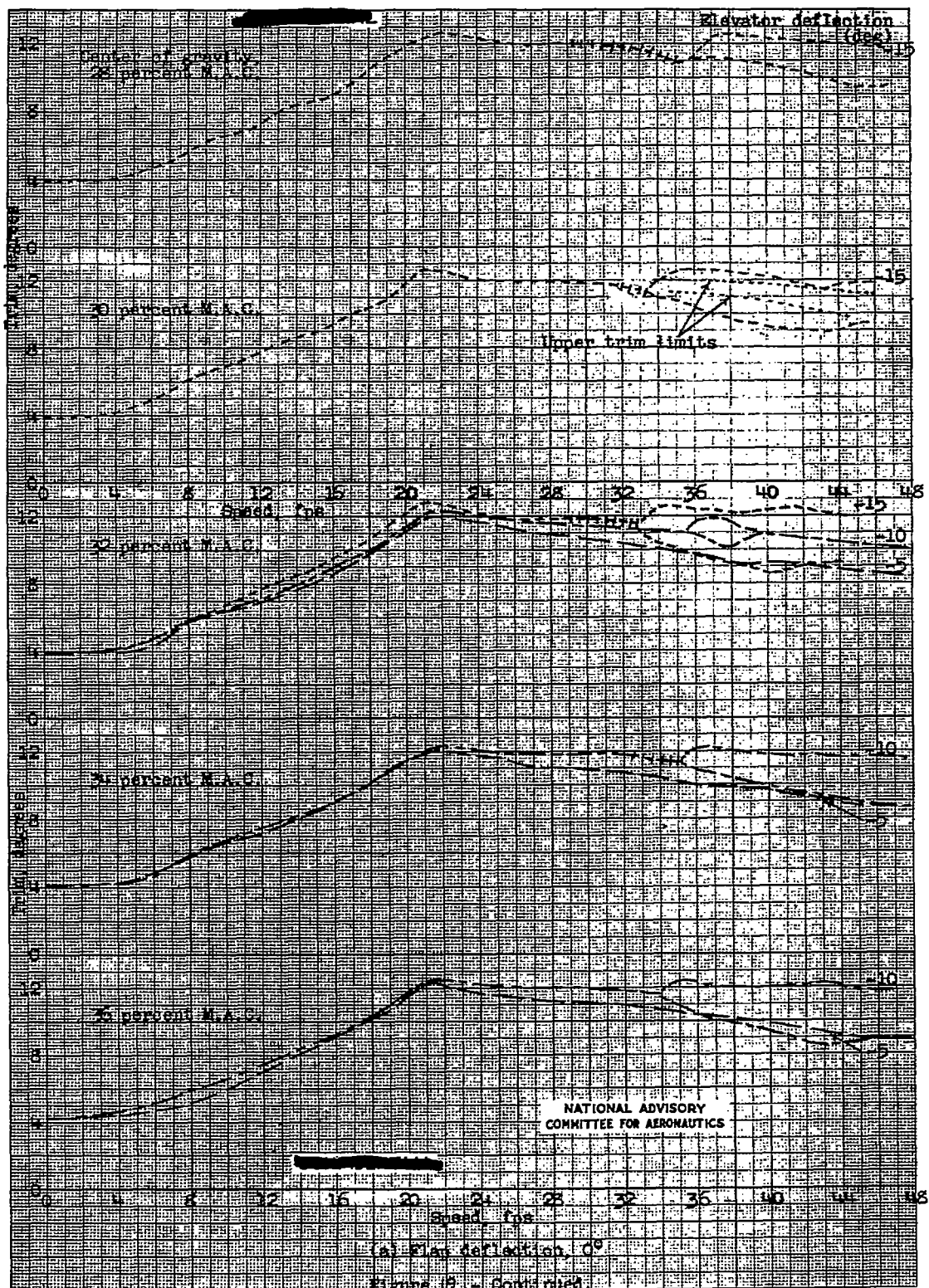


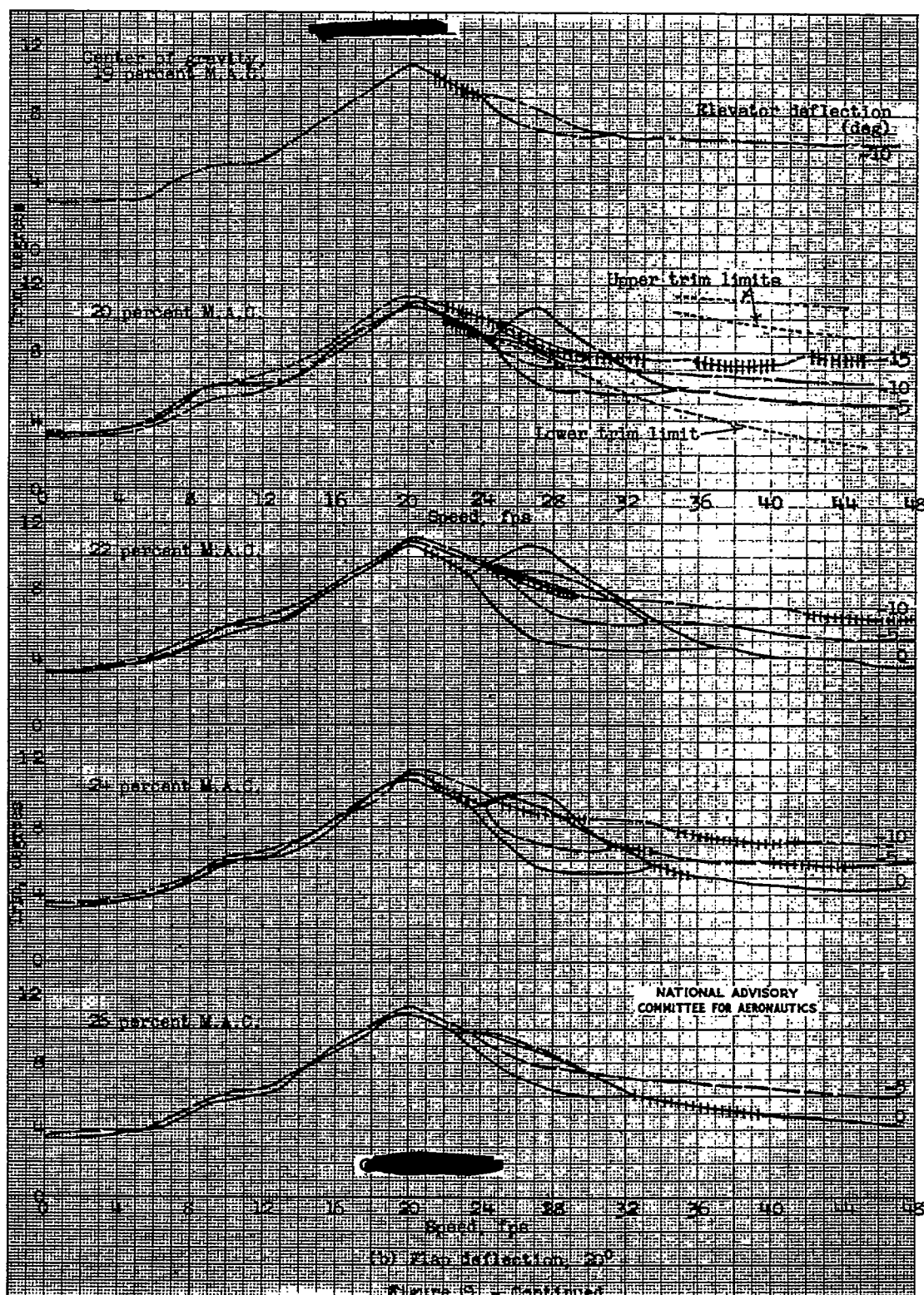






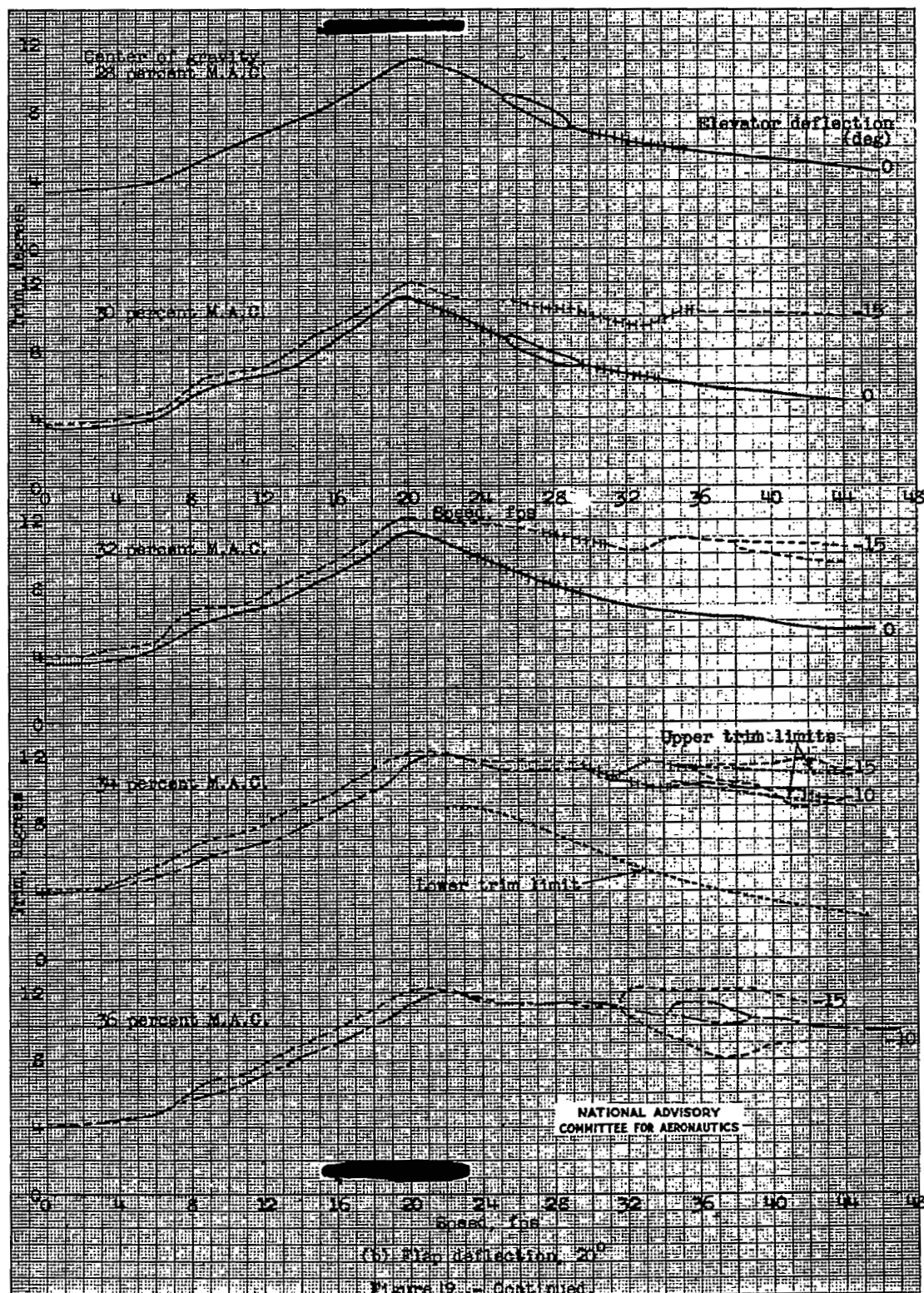


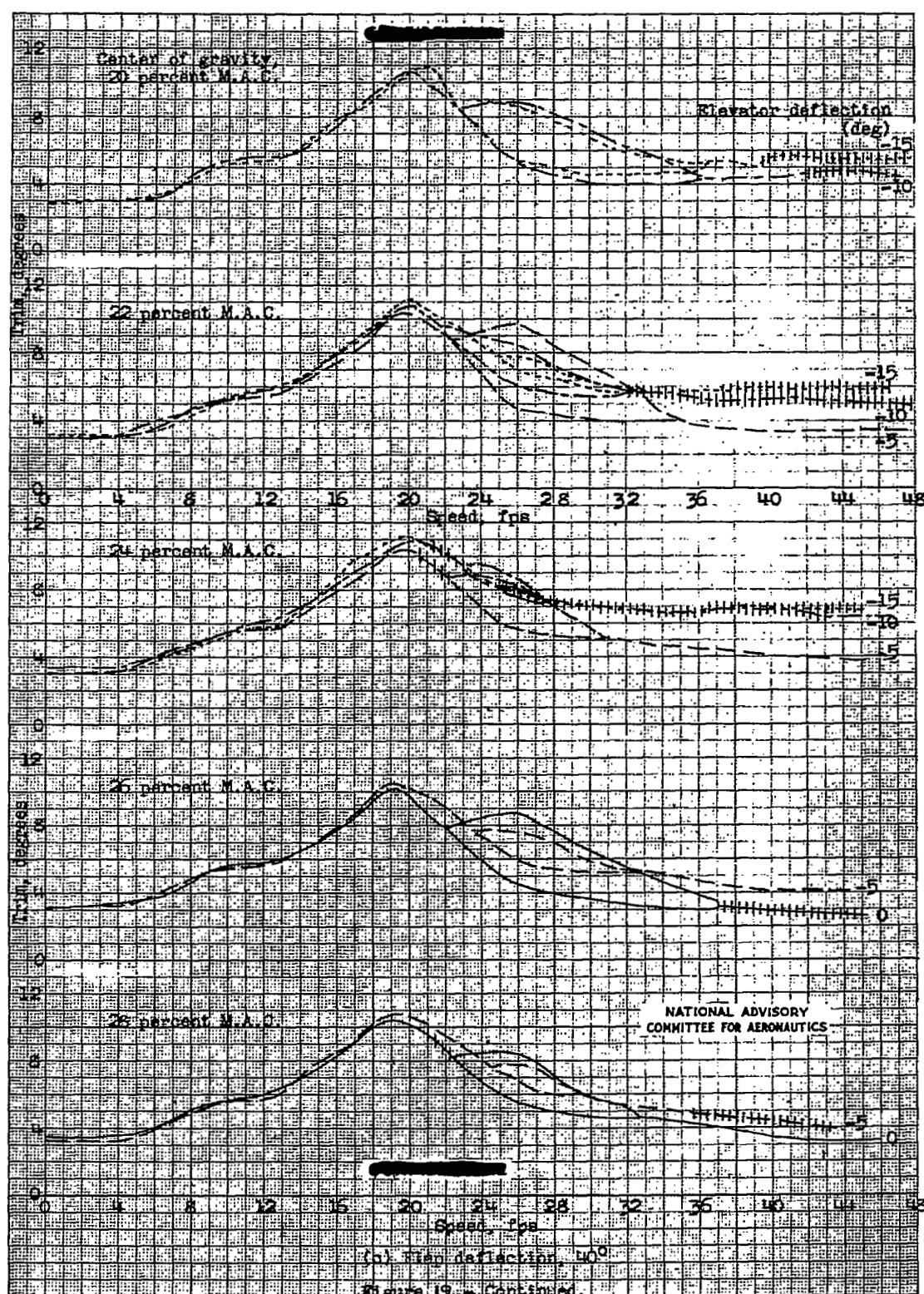


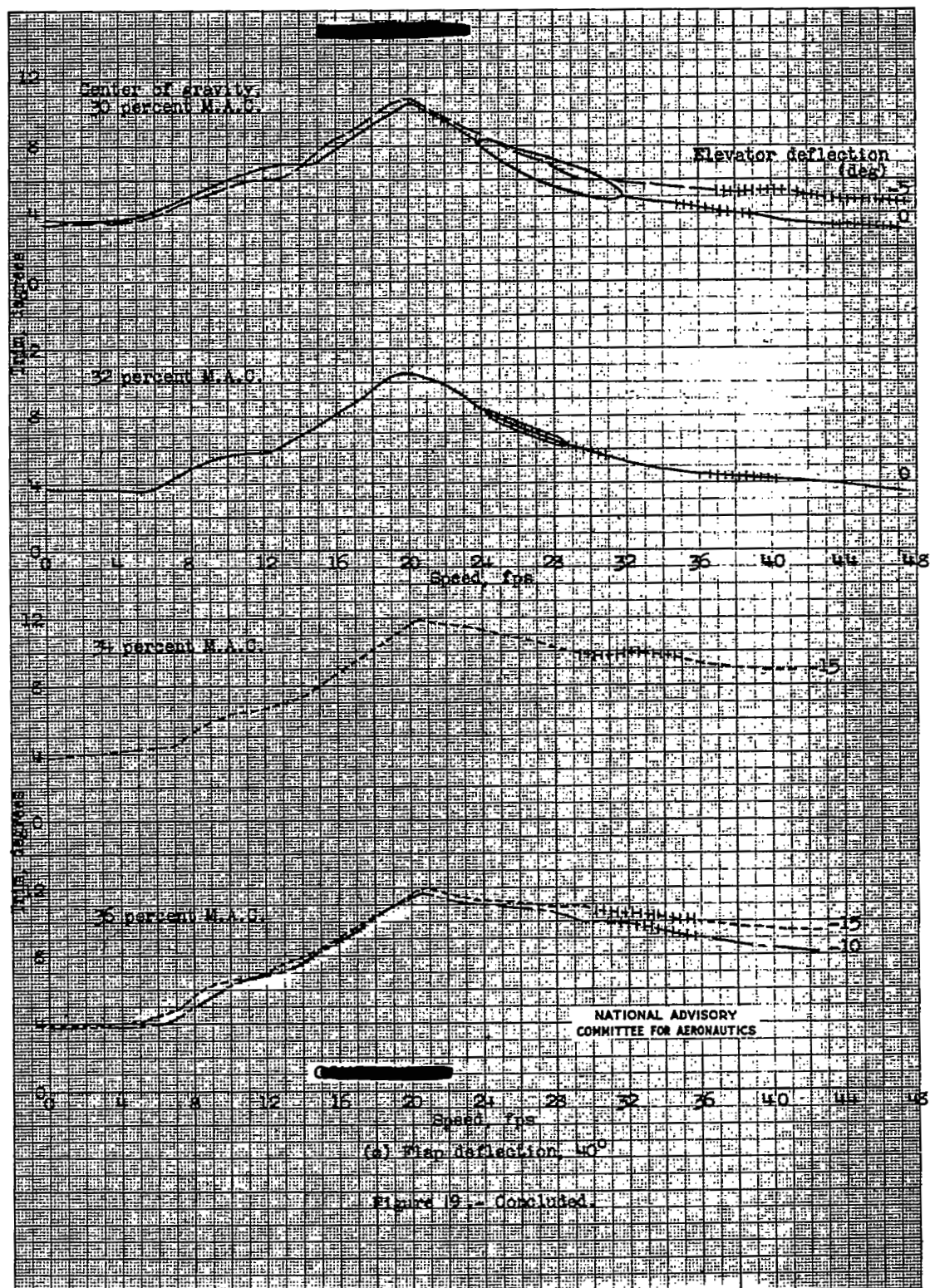


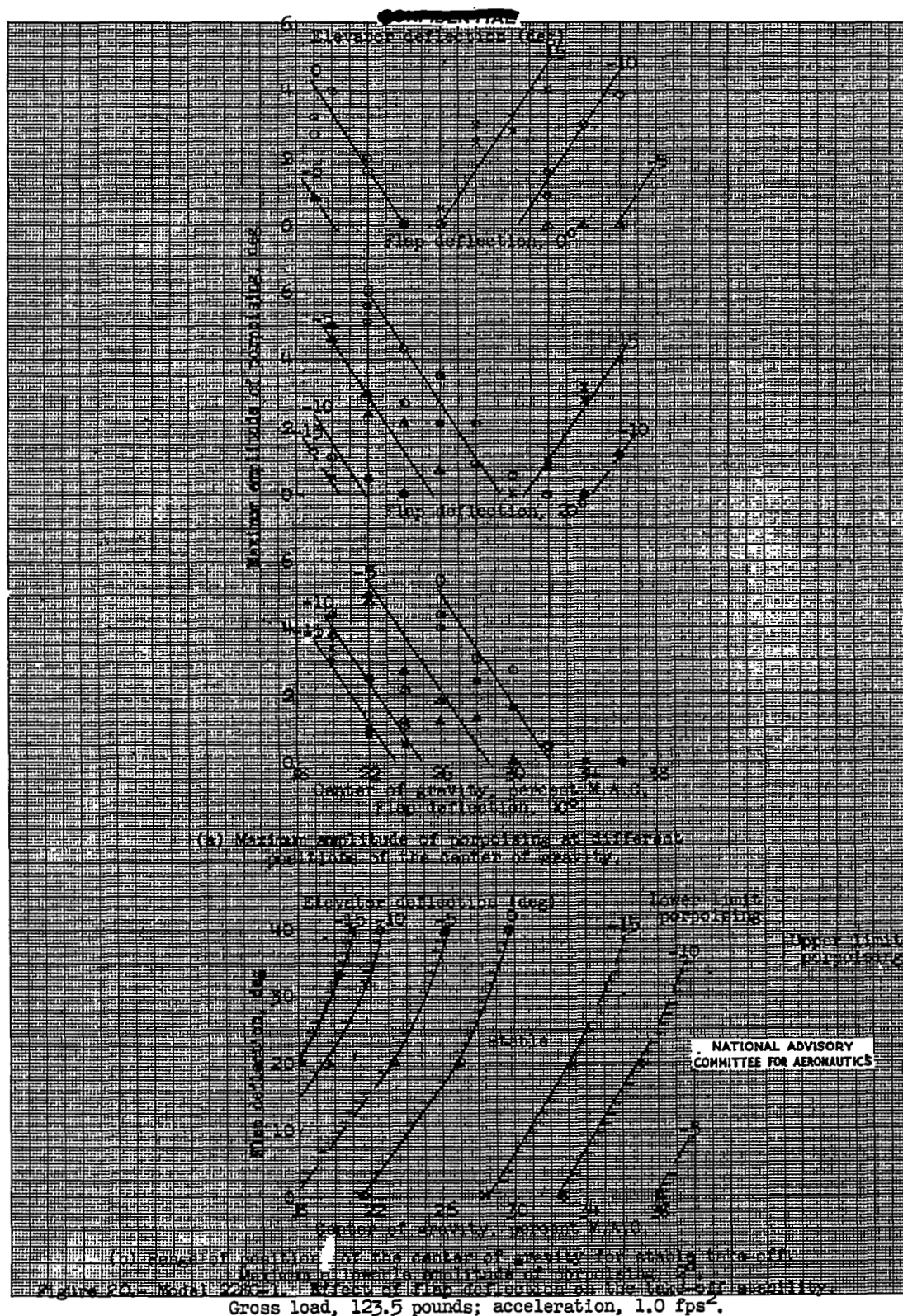
(b) Elevator deflection, 20°

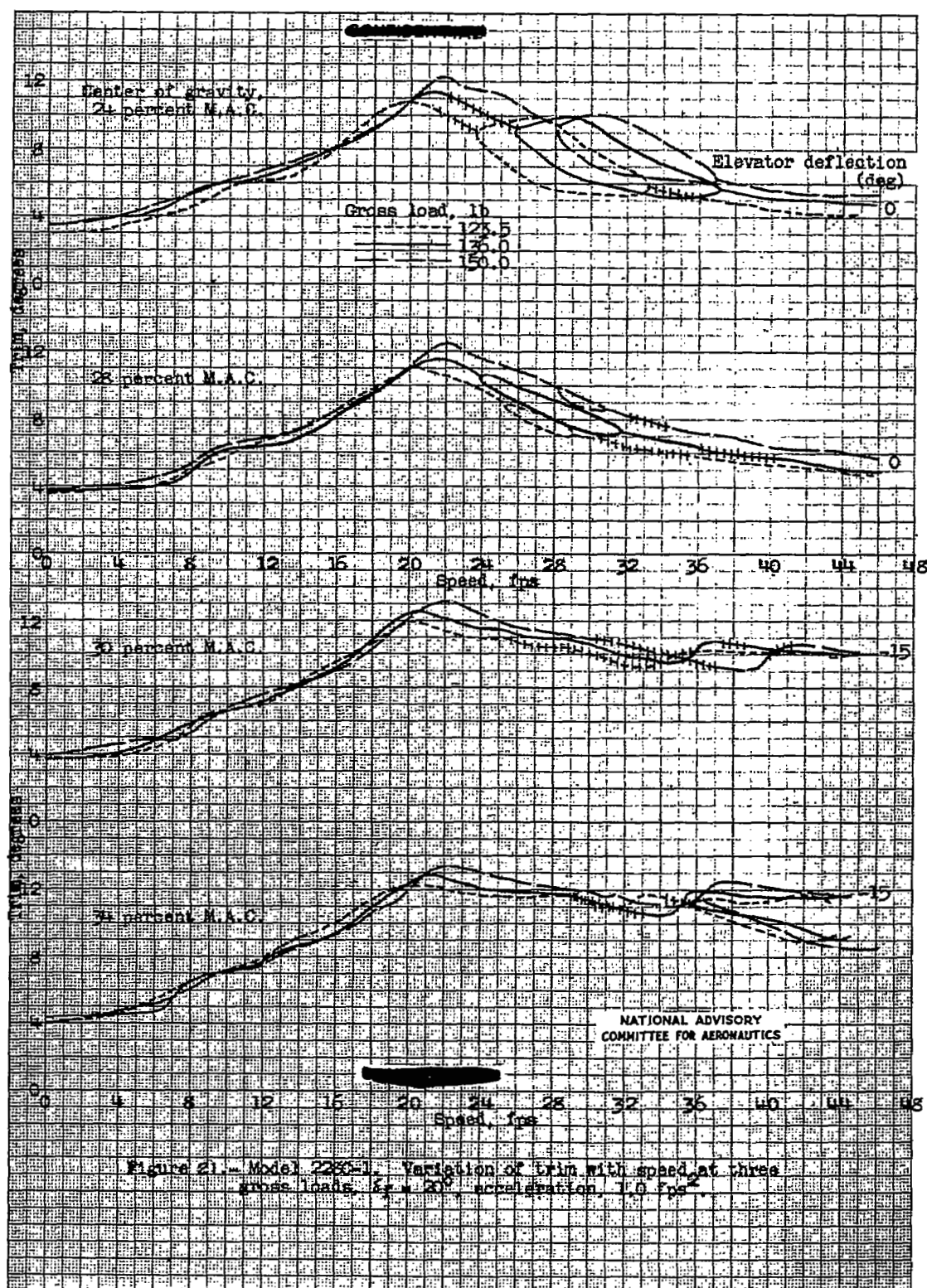
Figure 9.- Continued.

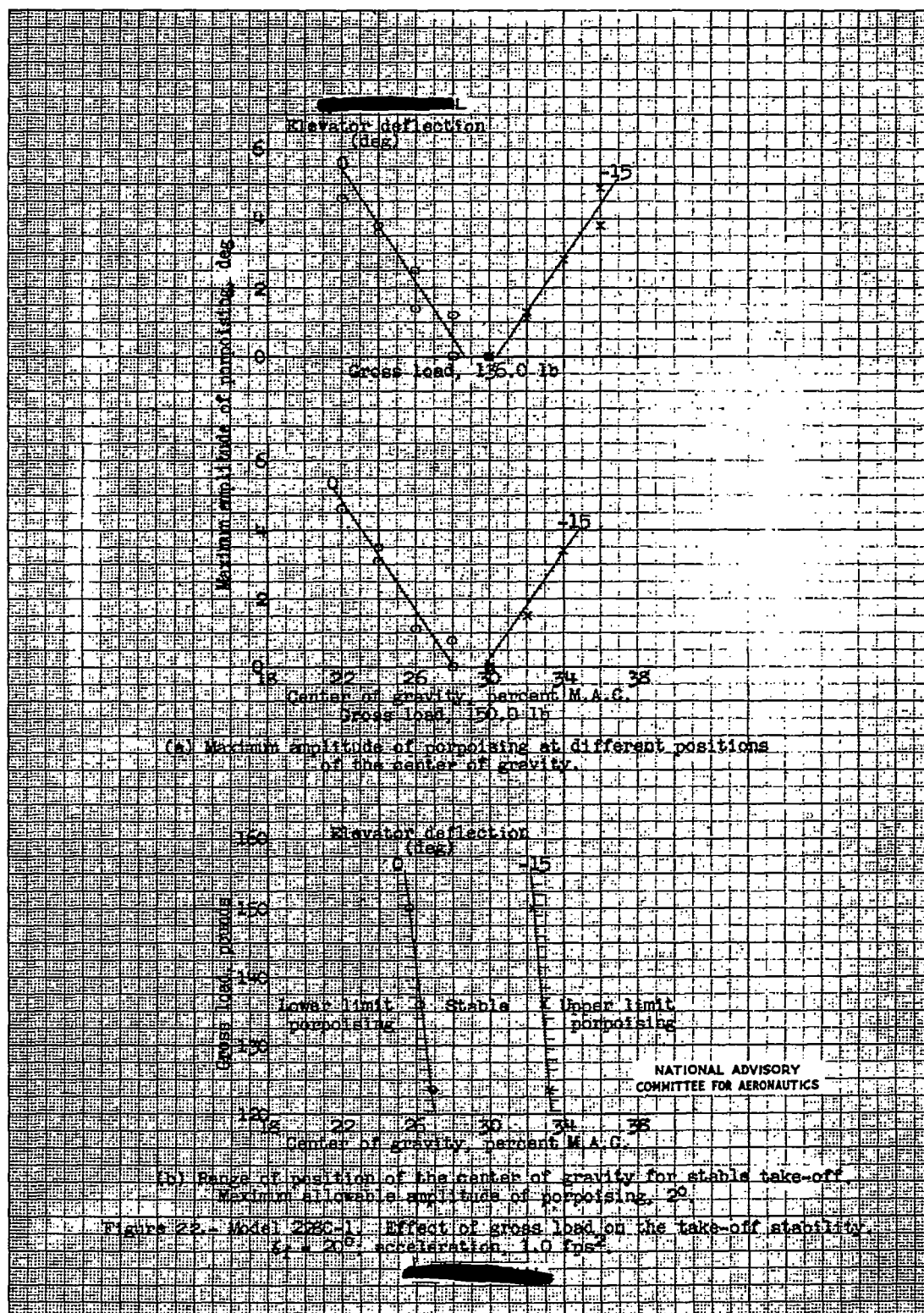


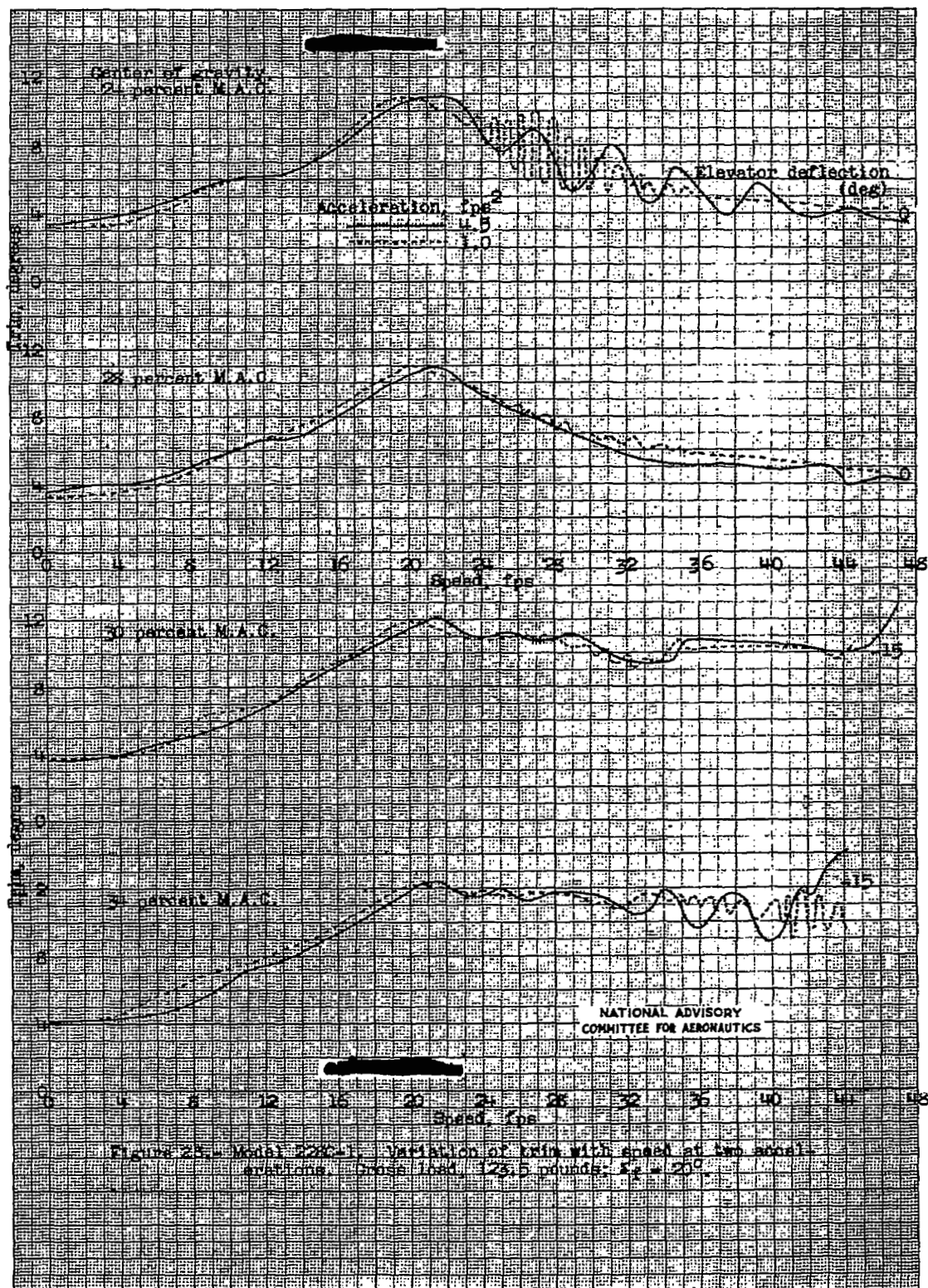


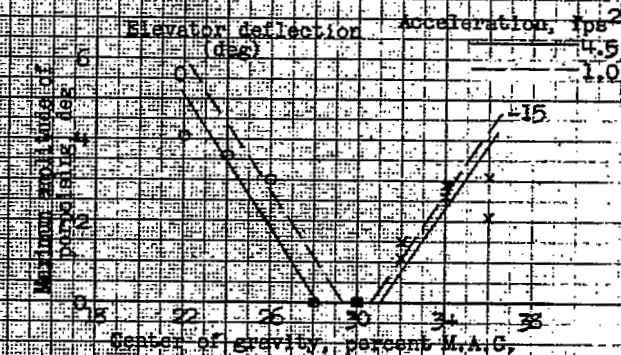




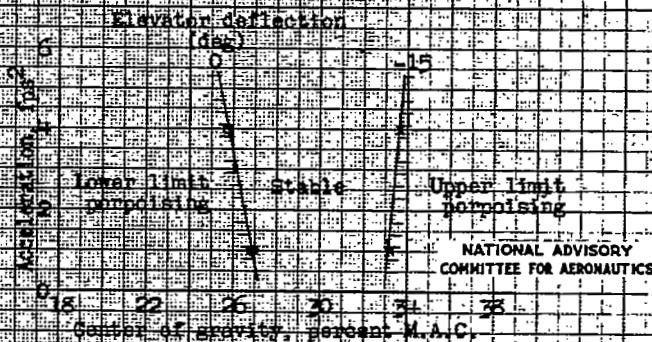






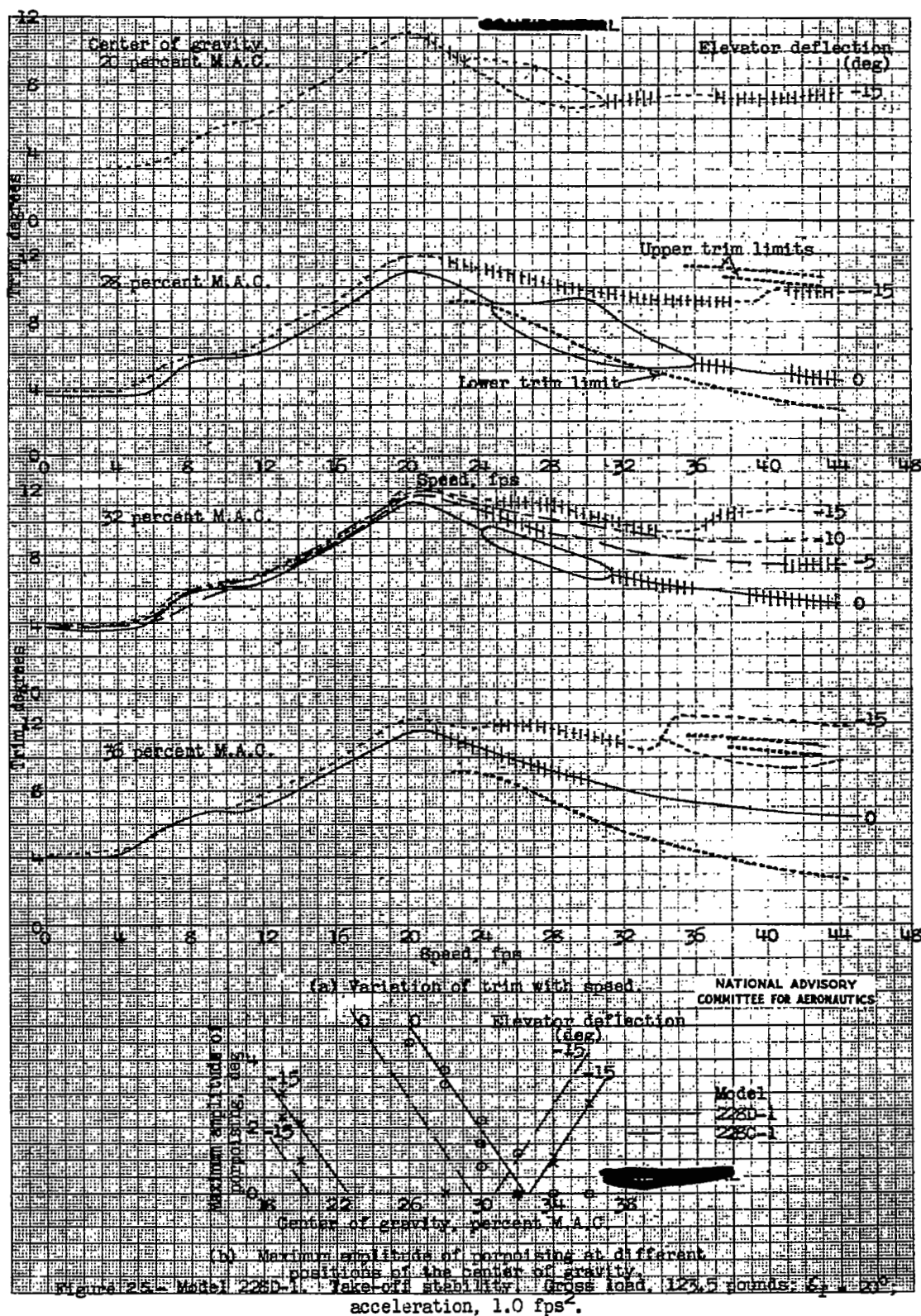


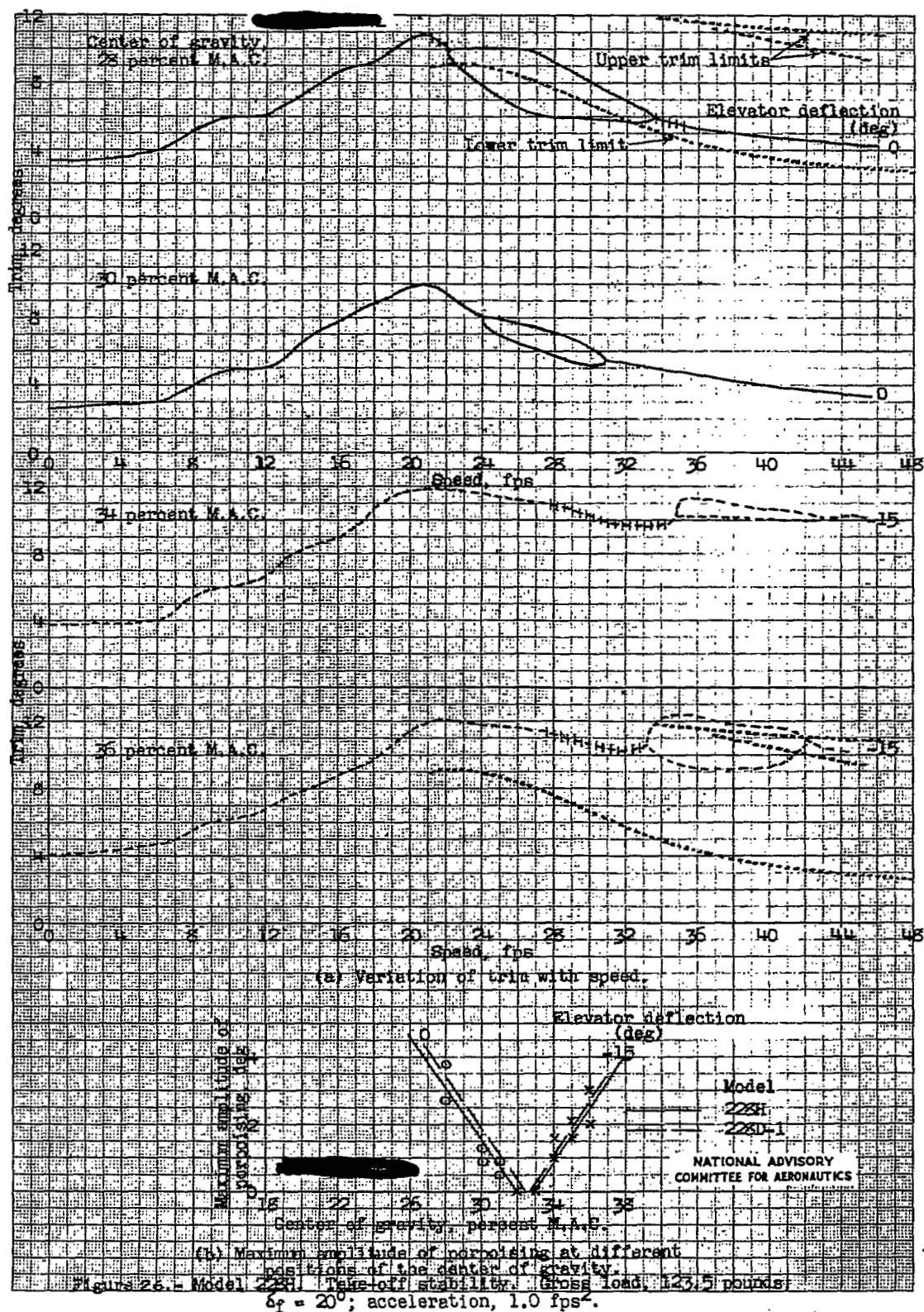
(a) Maximum amplitude of porpoising at different positions of the center of gravity

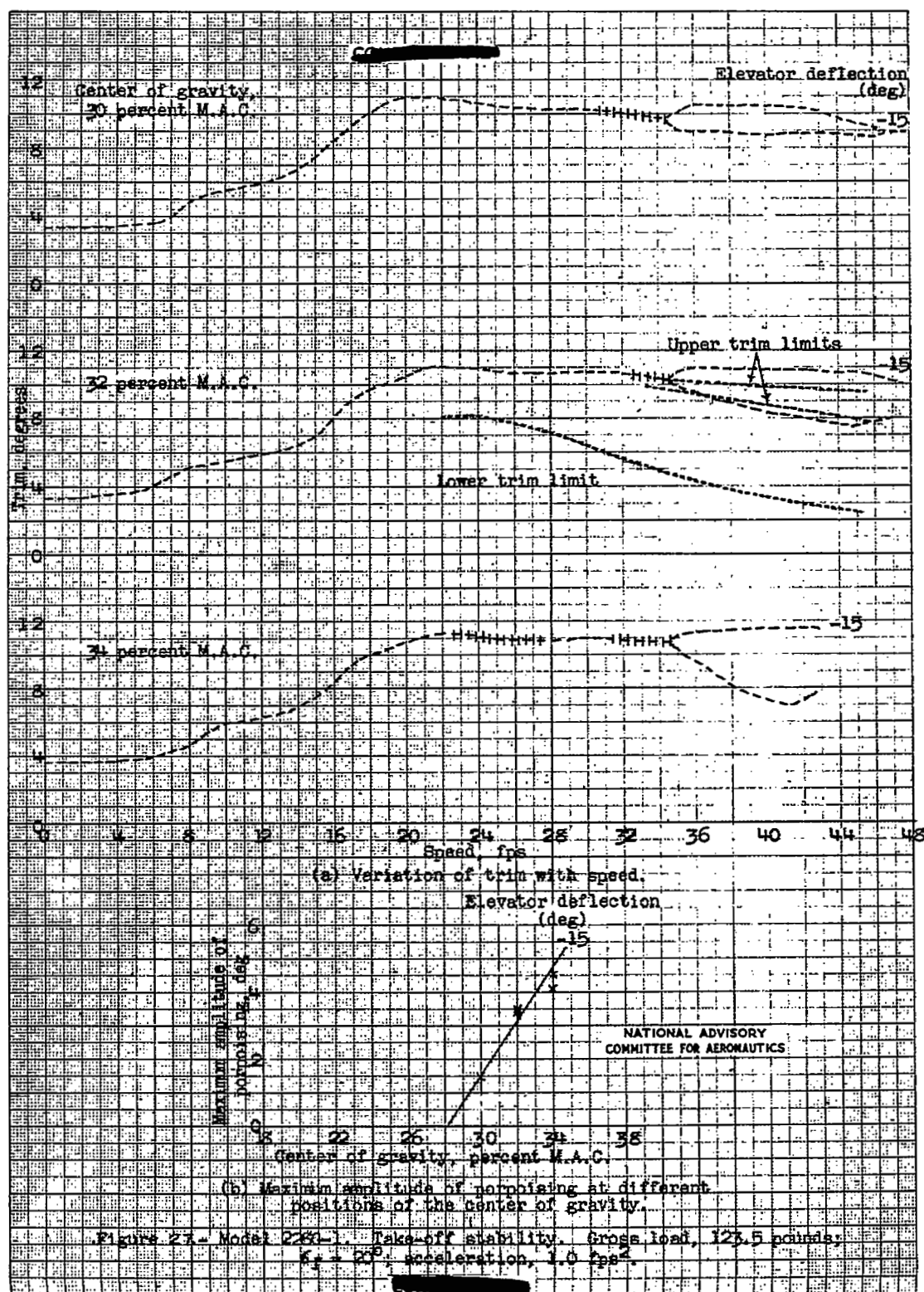


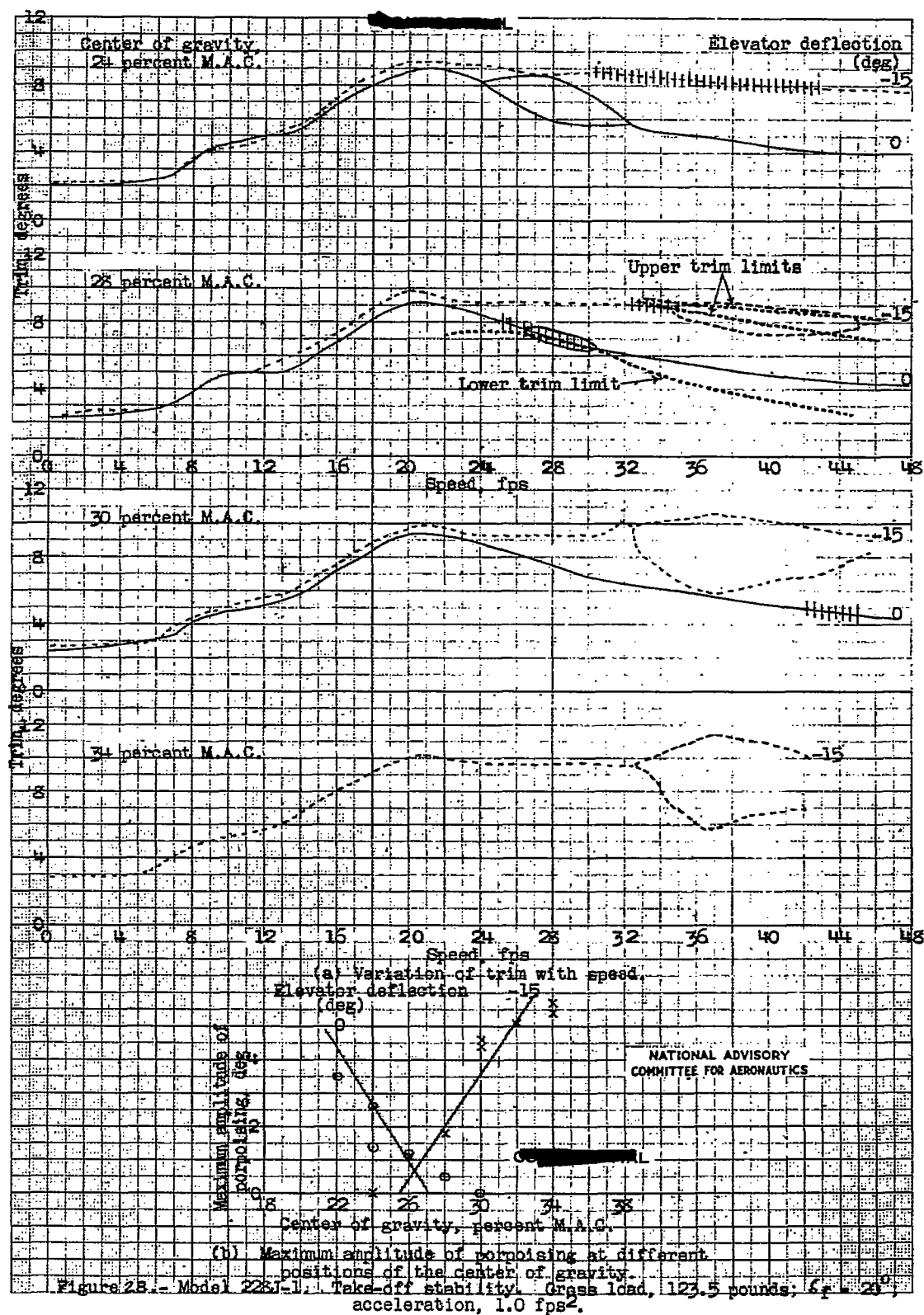
(b) Range of position of the center of gravity for stable take-off. Maximum allowable amplitude of porpoising, 2°.

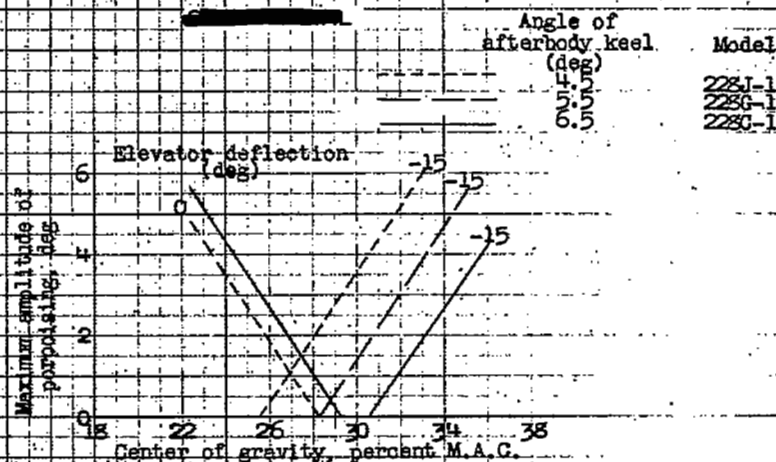
Figure 24. Model 28C-1. Effect of acceleration on the take-off stability. Gross load, 125.5 pounds;  $C_L = 20^\circ$



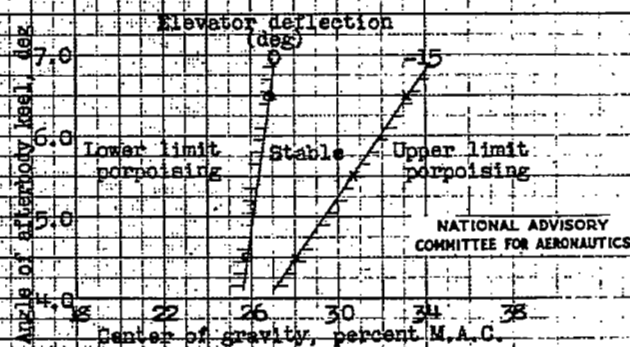






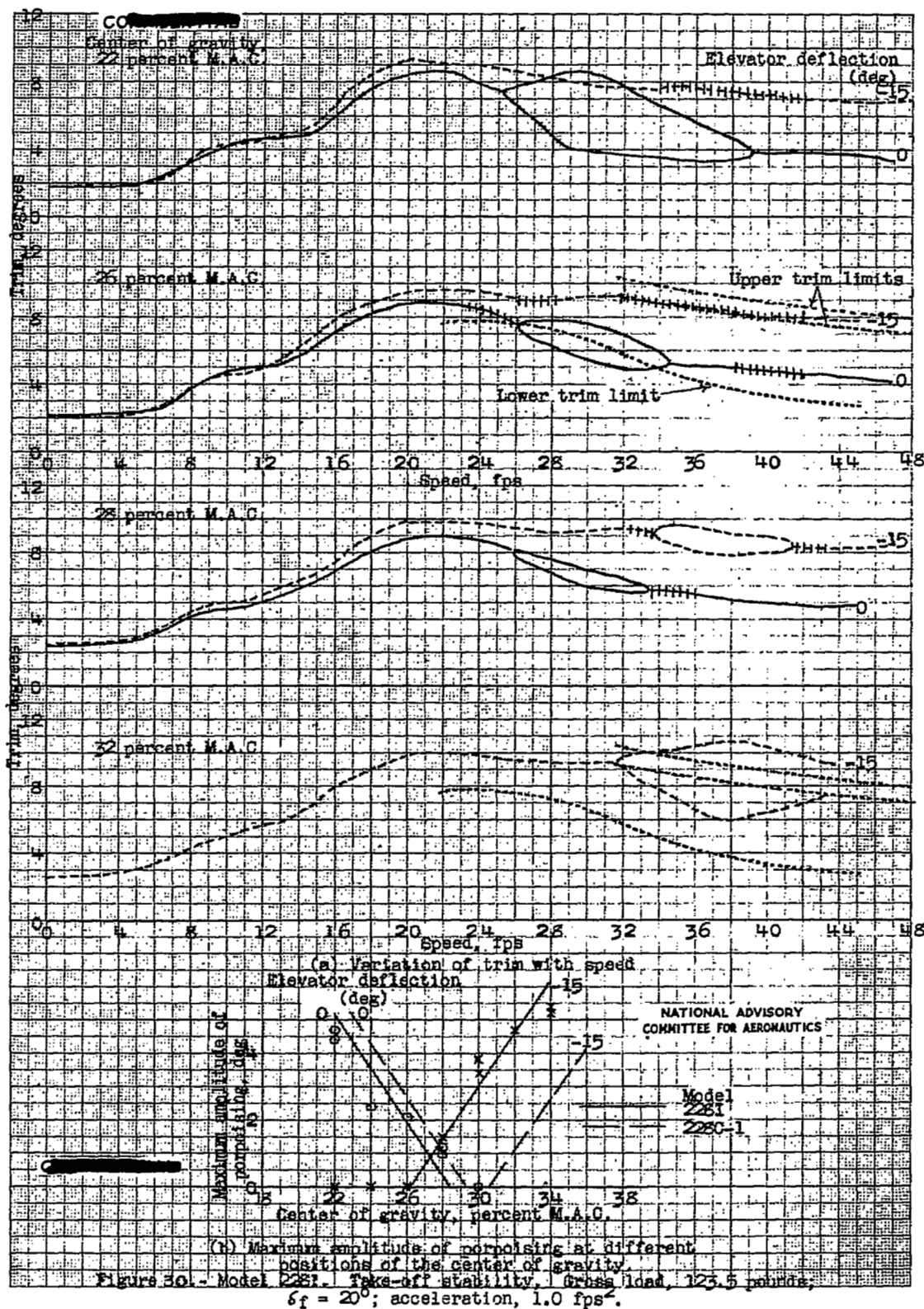


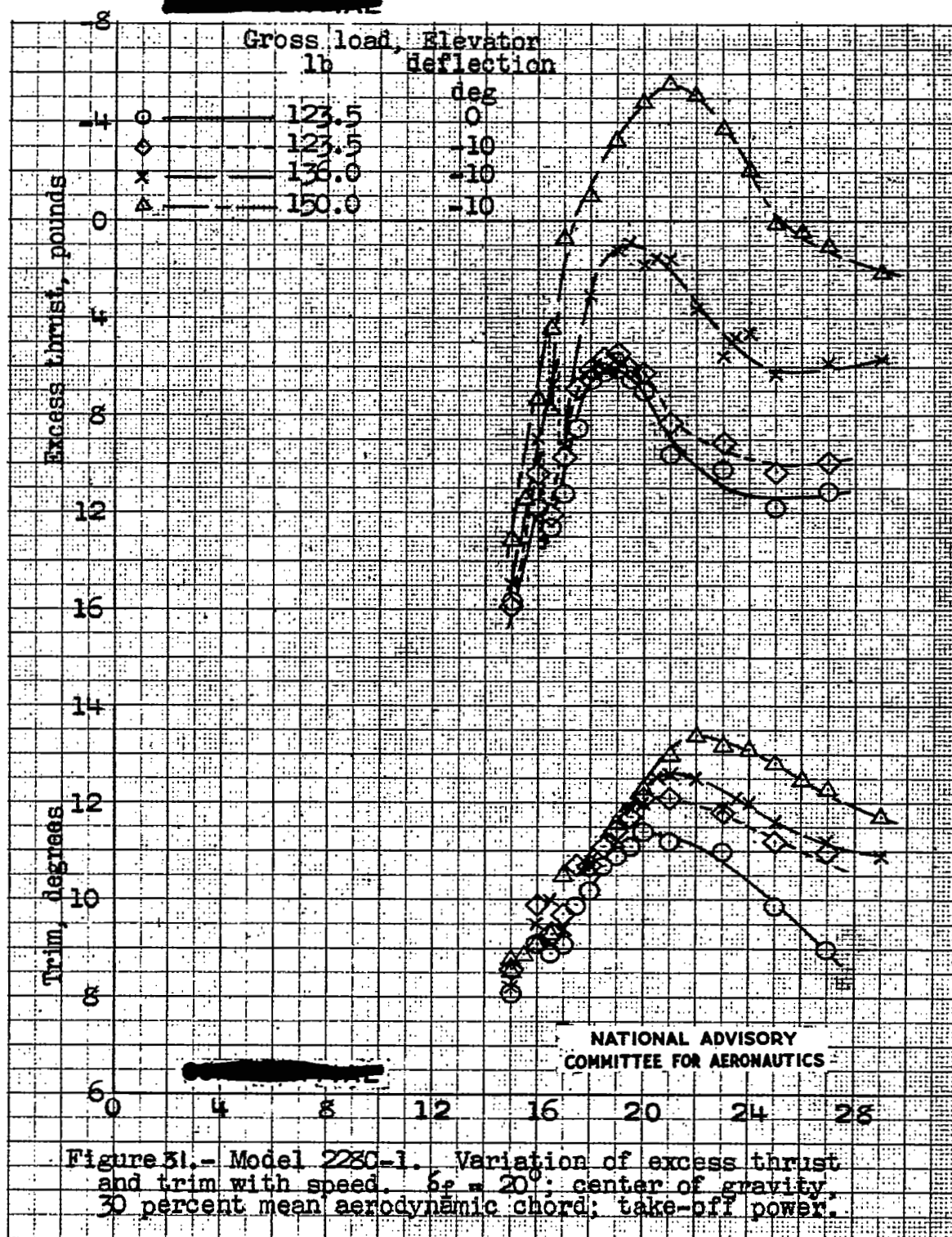
(a) Maximum amplitude of porpoising at different positions of the center of gravity.

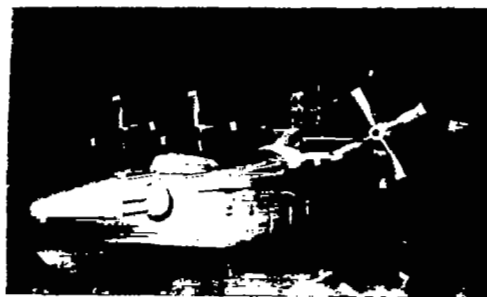


(b) Range of position of the center of gravity for stable take-off. Maximum allowable amplitude of porpoising, 20°.

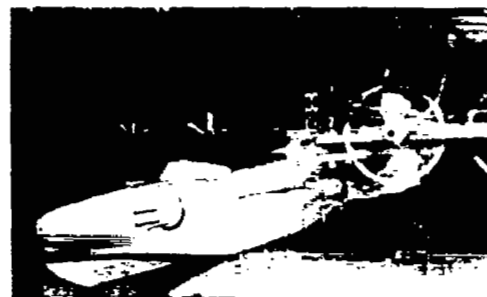
Figure 29. - Models 228C-1, 228G-1 and 228J-1. Effect of angle of afterbody keel on the take-off stability. Gross load, 123.5 pounds;  $\lambda_f = 20^\circ$ ; acceleration, 1.0 gps<sup>2</sup>.







Trim at rest,  $4.0^\circ$   
(Power off)



Trim at rest,  $2.3^\circ$   
(Take-off power)



Speed, 5 fps; Trim,  $3.0^\circ$



6.0 fps;  $3.0^\circ$



7 fps;  $3.8^\circ$

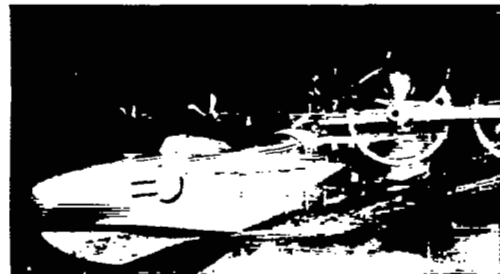


8 fps;  $4.1^\circ$

Figure 32.- Model 228J-1. Bow spray photographs. Flap deflection,  $20^\circ$ ; elevator deflection,  $0^\circ$ ; center of gravity, 34-percent mean aerodynamic chord; take-off power; gross load, 123.5 pounds.



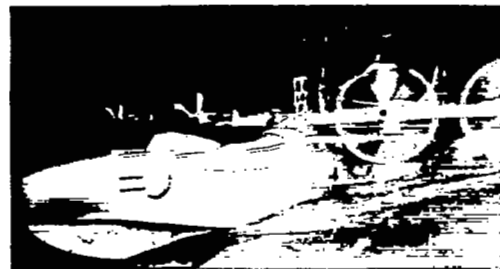
Speed, 9.0 fps; Trim,  $4.9^\circ$



10.0 fps;  $5.2^\circ$



11 fps;  $5.4^\circ$



12 fps;  $5.7^\circ$



13 fps;  $5.8^\circ$



14 fps;  $6.0^\circ$

Figure 32.- Model 228J-1, continued.

~~REDACTED~~ L



Speed, 15.0 fps; Trim,  $7.0^{\circ}$



16.0 fps;  $7.8^{\circ}$



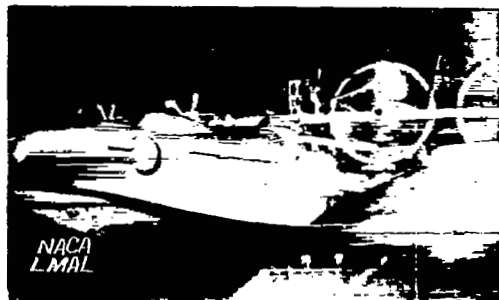
17 fps;  $8.0^{\circ}$



18 fps;  $8.0^{\circ}$



19 fps;  $8.7^{\circ}$

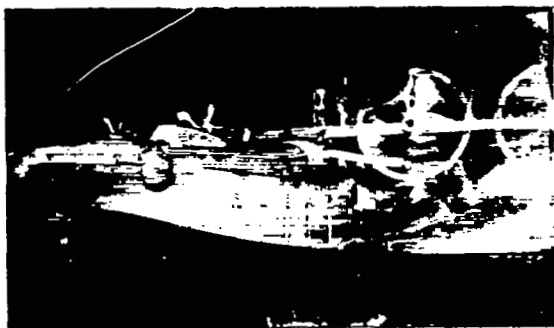


20 fps;  $9.1^{\circ}$

Figure 32.- Model 228J-1, continued.

~~REDACTED~~

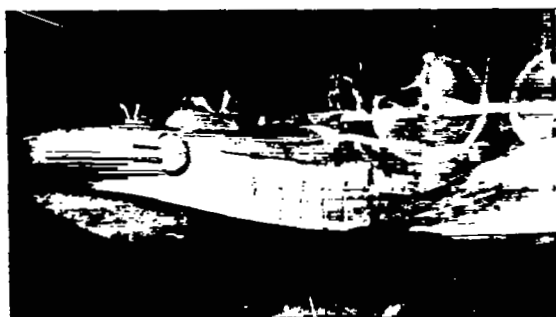
~~CONFIDENTIAL~~



Speed, 21.0 fps; Trim,  $9.2^\circ$



22.0 fps;  $9.3^\circ$



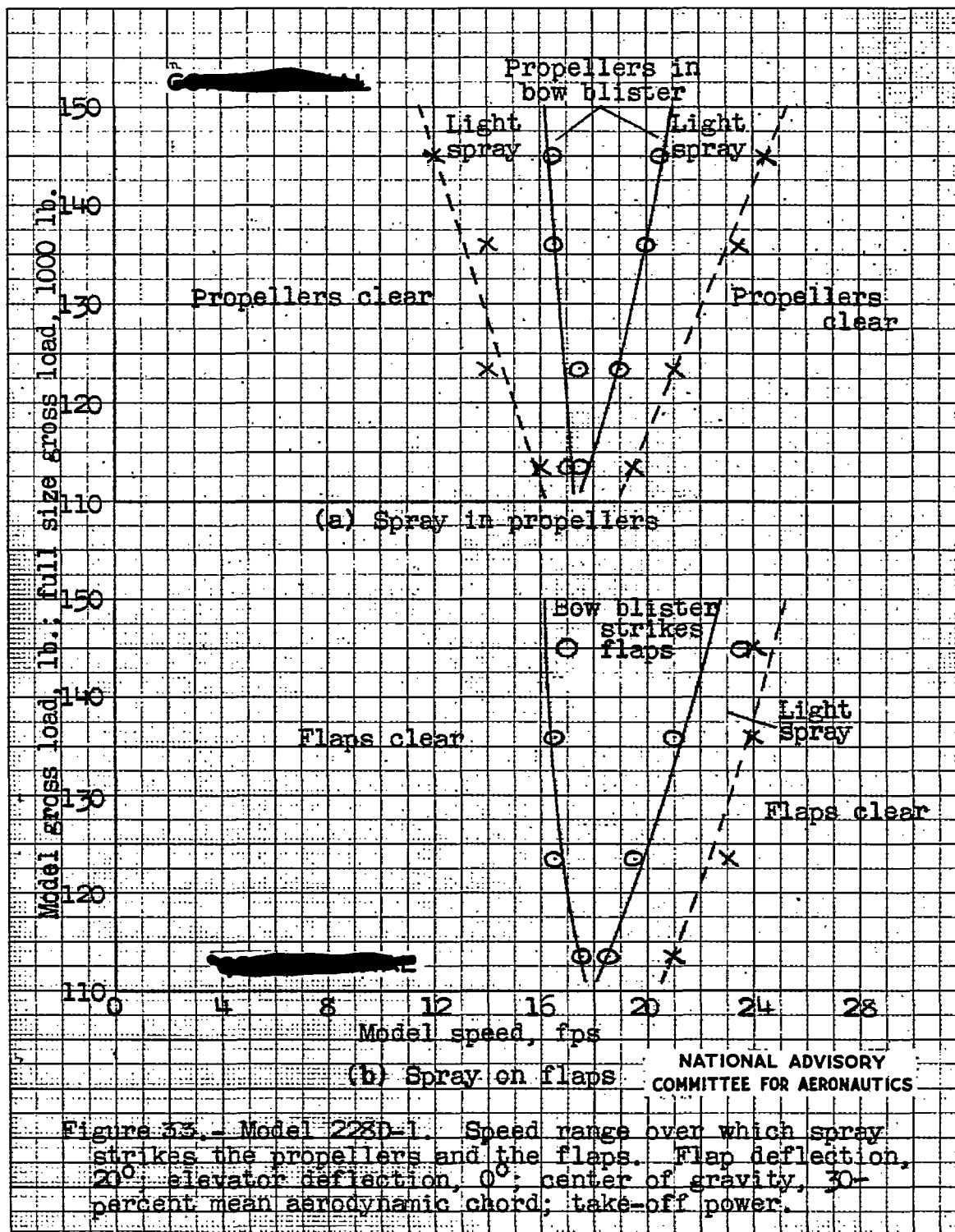
23.0 fps;  $9.4^\circ$

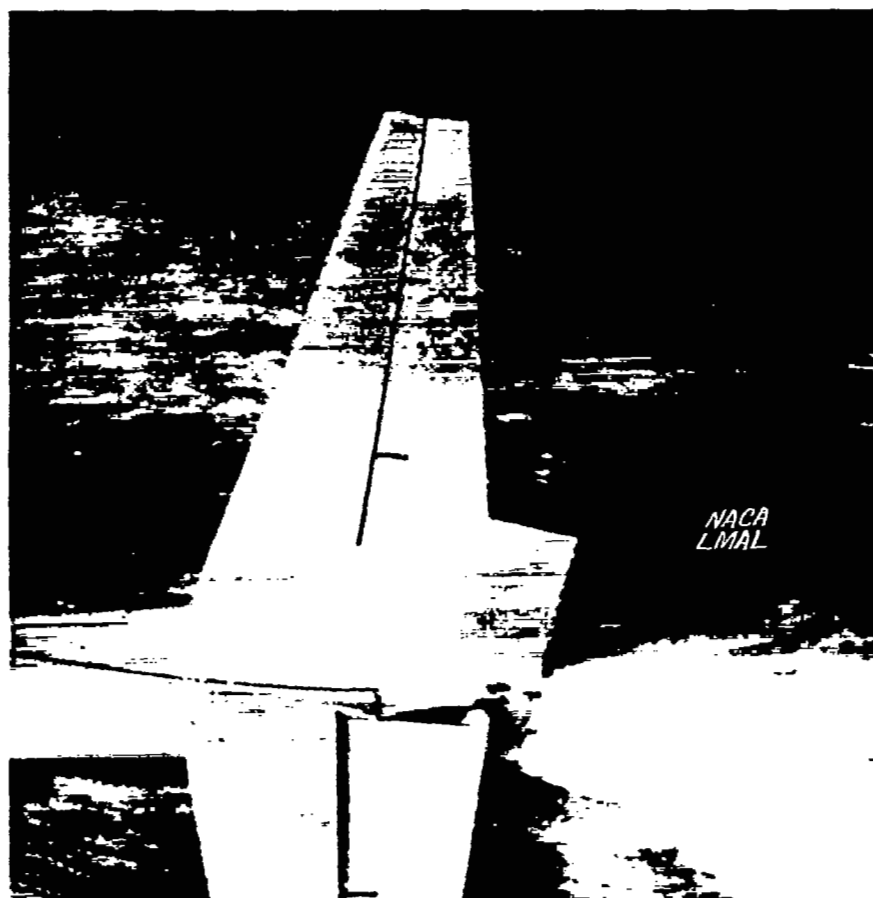


24.0 fps;  $9.3^\circ$

Figure 32.- Model 228J-1, concluded.

~~CONFIDENTIAL~~



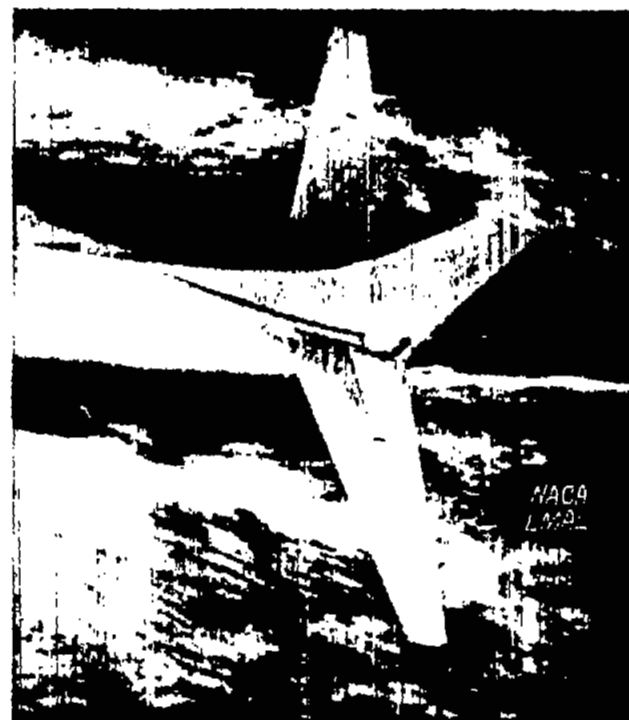


Speed, 19.5 fps  
Elevator deflection,  
 $-10^{\circ}$

Figure 34.- Model 228 C-1. Spray over tail turret near hump speed. Flap deflection,  $20^{\circ}$ ; center of gravity, 30-percent mean aerodynamic chord; take-off power; gross load, 123.5 pounds.

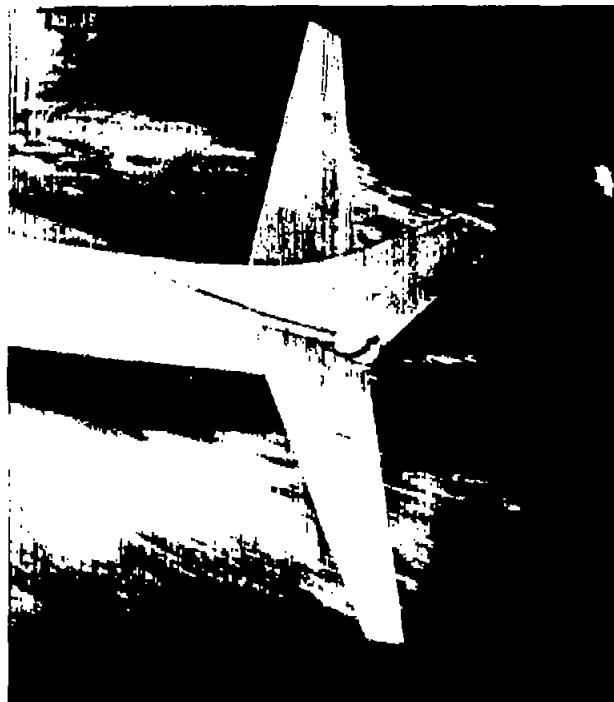


One-quarter take-off power  
Speed, 22.9 fps  
Trim,  $14.1^{\circ}$



Take-off power  
Speed, 21.0 fps  
Trim,  $12.0^{\circ}$

Figure 35.- Model 228 C-1. Effect of power on spray over tail assembly at speeds near hump. Flap deflection,  $20^{\circ}$ ; center of gravity, 30-percent mean aerodynamic chord; gross load, 123.5 pounds.



Spray under horizontal tail  
Speed, 34.0 fps  
Trim,  $10.5^\circ$



Spray over horizontal tail  
Speed, 36.0 fps  
Trim,  $10.5^\circ$

Figure 36.- Model 228 C-1. Spray on tail near upper trim limit of stability.  
Flap deflection,  $0^\circ$ ; center of gravity, 34-percent mean aerodynamic  
chord; take-off power; gross load, 123.5 pounds.

NASA Technical Library



3 1176 01436 3569